Functionalisation of graphene as a tool for developing nanomaterials with predefined properties

Abdelsattar O. E. Abdelhalim[1,2], Konstantin N. Semenov[3,1,4*], Dmitry A. Nerukh[5], Igor V. Murin[1], Dmitrii N. Maistrenko[4], Oleg E. Molchanov[4], Vladimir V. Sharoyko[3,1,4*]

[1]Institute of Chemistry, Saint Petersburg State University, 26 Universitetskii prospekt, Saint Petersburg, 198504, Russia

[2]Environmental Research Department, National Center for Social and Criminological Research (NCSCR), 4 Agouza, Giza 11561, Egypt

[3]Pavlov First Saint Petersburg State Medical University, 6–8 Lev Tolstoy Str., Saint Petersburg, 197022, Russia

[4]A. M. Granov Russian Research Centre for Radiology and Surgical Technologies, 70 Leningrad str., Saint Petersburg, 197758, Russia

[5]Department of Mathematics, Aston University, Birmingham, B4 7ET, United Kingdom

[*]Corresponding authors at: 6–8 Lev Tolstoy Str., Saint Petersburg, 197022, Russia (K. N. Semenov) and 26 Universitetskii prospekt, Saint Petersburg, 198504, Russia (V. V. Sharoyko)

E-mail addresses: knsemenov@gmail.com (K. N. Semenov), sharoyko@gmail.com (V. V. Sharoyko).

Abstract

Graphene based nanomaterials (GBN) have been recently applied in a broad range of science and technology fields such as nanobiomedicine, electronics, energy storage and power generation exploiting their unique electronic structure, physical properties, and opportunities for modifying their surface using covalent and non-covalent interactions. In the present review we systematised the origins of GBN functionalisation using organic and inorganic molecules, polymers, biomolecules, and anticancer drugs. We show that varying the procedure of GBN functionalisation allows to obtain nanomaterials with desired properties that can be applied to the development of materials with enhanced physicochemical properties, nanoplatforms for drug delivery, nanobiosensors for detection of various biomolecules, as well as nanomaterials for bioimaging and diagnostics. The review can be useful for experts in the fields of material science and nanobiomedicine.

Keywords: graphene, graphene oxide, functionalization, nanobiomaterials, drug delivery, nanobiosensors, bioimaging.

1. Introduction

Graphene based nanomaterials (GBN) such as graphene oxide (GO), graphene, and reduced graphene oxide (rGO) have been at the forefront of research due to their unique structure and distinguished physico-chemical properties (Table 1). One of the most important application of GBN is biomedicine: tissue engineering [1], bioimaging [2,3] targeted anticancer drug delivery [4–9], biosensors [10–12], development of antiviral [13–16], antibacterial [17–20], antifungal materials [21,22], as well as the delivery of biomolecules such as enzymes [23,24], proteins [25–27], genes [28–30], RNA [31,32], and DNA [33,34]. In addition, GBN were used as materials for energy applications (fuel cells [35,36], batteries [37,38], solar cells [39,40]), for manufacturing smart materials [41], nano-enhancers to design heat transfer media with better thermal performance [42–44] and for water disinfection and desalination [45–47]. Fig. 1 summarises the publications distribution in these research areas.

GBN can be functionalised through covalent [48–52] and non-covalent [53–57] interactions. Functionalisation of GBN leads to the enhancement of their electrical [58,59], optical [60,61], thermal [62,63], electronic [64–66], and mechanical [67,68] properties. Graphene is a monolayer carbonaceous material [69] that can be prepared in the form of single or multilayered flakes depending on the method of preparation [70]. It can be synthesised using various methods such as chemical vapour deposition (CVD) [71–77], electrochemical exfoliation of graphite [78–83], mechanochemical exfoliation of graphite [84] as well as chemical and thermal reduction of GO resulting in the formation of rGO [85–91].

Graphene is composed of sp^2-hybridised hexagonal carbon atoms forming two-dimensional nanolayers, while GO contains various oxygen functional groups distributed on the surface such as carboxyl, carbonyl, and lactol at the edges of GO layers in addition to epoxy and

hydroxyl groups on the basal plane [92–97], (Fig. 2). rGO is a form of GO in which most of the oxygen-containing functional groups are reduced by such agents as hydrazine hydrate or biomolecules [98,99].

A single layer of graphene was isolated in 2004 by Andrei Geim and Konstantin Novoselv [100], while GO was synthesised for the first time in 1859 by Benjamin Brody by oxidising graphite using a mixture of oxidising agents potassium chlorate and fuming nitric acid [101]. However, the most efficient method was developed by William Hummers and Richard Offeman in 1957 using the oxidising mixture of sulphuric acid, sodium nitrate, and potassium permanganate [102].

This review summarises approaches for the covalent and non-covalent functionalisation of GBN. Due to multifunctional groups located on the GO surface as well as the presense of sp^2-hybridised carbon atoms, further functionalisation of GBN can be conducted with the molecules of various nature. A multitude of organic reactions (Fig. 3) can be carried out: amidation, esterification, 1,3-dipolarcycloaddition, halogenations, as well as hydrogen bonding, π–π stacking interactions, and hydrophobic interactions.

These reactions allow to obtain unique materials for biomedical applications, such as cancer treatment [103], drug and biomolecules delivery [104,105], development of biosensors [106] and materials with antiviral [107], antibacterial [108], and antifungal properties [109]. This review demonstrates that among GBN, GO has the highest potential for the applications in nanomedicine due to the following reasons. (*i*) GO consists of various functional groups which allow to perform further functionalisation of the surface. (*ii*) The functionalisation of GO increases its biocompatibility. (*iii*) The presence of oxygen-containing functional groups provides the stability of GO aqueous dispersions.

2. Functionalisation of GBN

2.1 Graphene conjugation with organic molecules

Graphene structure can be covalently or non-covalently functionalised with organic molecules using amidation, esterification, and halogenation reactions. Hossain et al. [110] studied the diazotisation of graphene obtained by epitaxial growth method (G-epitaxial) on SiC. The authors demonstrated that the basal plane of graphene can be functionalised with such organic molecule as 2-aminoethanethiol ($HS\text{-}C_2H_4\text{-}NH_2$) using diazotisation reaction. In addition, it was found that amine diazonium salts undergo spontaneous reduction resulting in functionalisation of the graphene surface with $HS\text{-}C_2H_4$ residues leading to G-thioethyl (GT). In their further work [111] Hossain et al. performed the covalent immobilisation of AuNPs on the surface of GT. The −SH-groups of GT were treated with $HAuCl_4$ with subsequent reduction by $NaBH_4$. Thus, Au was covalently attached to graphene through −S−Au bond. Then, the immobilised AuNPs were modified with such sulphur-containing molecules as hexanedithiol ($HSC_6H_{12}SH$). The resulting assembly with graphene can be used for loading various sulphur-containing biomolecules through the formation of an Au-S linkage (Fig.4).

Wang et al. [112] developed a covalent functionalisation with 3-aminopropyltriethoxysilane (APTS) through the hydroxyl groups on the graphene surface using DCC as a catalyst (Fig. 5). De Sousa et al. [113] presented the covalent functionalisation of GO with mannosylated ethylenediamine, the reaction proceeded through EDC/NHS coupling (Fig. 6). Shang et al. reported that GO was covalently functionalised with N-heterocyclic carbene–palladium complex ($NHC\text{-}Pd^{2+}$) for the application as an efficient catalyst for Suzuki–Miyaura coupling reactions [114].

Qian et al. presented the procedures of covalent functionalisation for graphene quantum dots where graphene surface was functionalised with organic molecules including dialcohols, diamines, and dithiols for bioimaging applications [115]. Yu et al. performed DFT study of non-covalent interaction between graphene and some aromatic molecules including thiophene (T), benzene (B) and pyridine (P). According to the study the aromatic rings of these molecules were placed on the top of the graphene surface at the height of 0.35 nm in parallel or vertical orientation. The results demonstrated that the interaction between the two polar molecules (T, P) and graphene is weaker than that of the nonpolar molecule (B). In addition, the non-covalent interactions between the aromatic molecules and graphene surface mainly originates from the π–π stacking between the π electrons of aromatic compound and graphene [116].

2.2 Graphene conjugation with inorganic molecules

Graphene surface can be functionalised with inorganic molecules including metal and metal oxide nanoparticles. Poh et al. [117] developed a method of graphene's halogenation (Fig. 7) through the covalent attachment of chlorine, bromine, or iodine. In this method graphite oxide (GrO) was prepared from graphite by oxidation followed by the thermal exfoliation of GrO with the formation of rGO (TRGO).The obtained nanomaterials can be used in the development of electronic and electrochemical devices.

Lai et al. [118] presented the synthesis of brominated graphene via electrophilic substitution reaction using N-bromosuccinimide (NBS) in aqueous solution of sulfuric acid to stimulate the decomposition of NBS and facilitate the formation of bromine cations. Then, these cations acted as electrophiles and covalently bonded to the defect sites of rGO (mostly sp^2 C–H) located at the edges of graphene flakes. The authors introduced a reaction mechanism based on the electron exchange reaction. It is well known that carbon atoms of the rGO lattice are

electron-rich due to sp^2 -hybridisation and they possess negative partial charge while bromine cations are electron-deficient and therefore possess partial positive charge. Thus, the generated bromine cations could be covalently attached to the defects of rGO (Fig. 8).

Dong et al. demonstrated the possibility of the reaction between GO and $FeCl_3$ [119]. Coordination bonds were formed between Fe^{3+} and hydroxyl groups of GO at the edges of the flake (Fig. 9). Literature analysis shows that GBN were non-covalently functionalised with metal nanoparticles for biosensing and antibacterial applications, for instance, silver nanoparticles (AgNp) [120–128], gold nanoparticles (AuNp) [129–136], and platinum nanoparticles (PtNp) [137–142]. In addition, the non-covalent functionalisation of GBN with metal oxide nanoparticles (ZnO [143–146], CuO [147,148] allows to obtain nanomaterials for the development of antimicrobial pharmaceutics and biochemical sensors for single stranded RNA detection. At the same time, covalent and non-covalent functionalisation of GBN with Fe_3O_4 magnetic nanoparticles allow to obtain nanomaterials for drug delivery and cancer sensing [149–154] (see Table 2).

2.3 Graphene conjugation with polymers

Graphene and GO can be functionalised with various polymers through covalent [155] and non-covalent interactions [55]. The obtained nanomaterials can be used in energy applications, catalysis, and biomedicine [156–158]. Fang et al. [159] performed the covalent functionalisation of graphene nanosheets with linear polystyrene (PS, M= 60 kDa) for preparing nanocomposites with enhanced mechanical properties (increased tensile strength and Young's modulus by 70% and 57% in comparison with individual PS). At first, the authors prepared GO using modified Hummers and Offeman's method then reduced it using hydrazine hydrate to rGO sheets. Then, hydroxylated graphene (G-OH) was synthesised *via* diazonium addition reaction in

the presence of 2-(4-aminophenyl) ethanol and isoamyl nitrite. The obtained G-OH was treated with triethanolamine and 2-bromopropionyl bromide to prepare graphene-based initiator. Finally styrene was added to the graphene-based initiator in the presence of methyl-2-bromopropionate (MBP), CuBr and N,N,N′,N′,N″-pentamethyl-diethylenetriamine (PMDETA) to synthesise polystyrene covalently functionalised with graphene nanosheets (Fig. 10).

Cano et al. [160] demonstrated the possibility of covalent functionalisation of GO with poly(vinyl alcohol) (PVA) for enhancing the mechanical properties of PVA. As a result, the authors demonstrated 60% improved Young's moduli and 400% tensile strength compared to non-modified PVA. The authors performed carbodiimide coupling of GO with (PVA, M= 6-500 kDa) using N,N'-dicyclohexylcarbodiimide (DCC) and 4-dimethylaminopyridine (DMAP) to produce GO-PVA conjugate (Fig. 11). Wan et al. [161] performed the covalent functionalisation of GO surface with diglycidyl ether of bisphenol-A (DGEBA) (Fig. 12), resulting in the formation of (DGEBA–GO) polymers with improved thermal stability and mechanical properties such as enhanced tensile strength (61–75% increase) and fracture toughness (29–41% increase) compared to non-modified DGEBA.

Xu et al. [162] demonstrated the covalent functionalisation of GO with 6-armed PEG-NH_2. At first the authors converted 6-armed PEG−OH to 6-armed PEG with six amino end groups (6-armed PEG-NH_2) according to the protocol applied by Mei et al. [163] with subsequent covalent functionalisation of GO surface by 6-armed PEG-NH_2 through amidation reaction using EDC·HCl as a coupling agent. The obtained nanomaterial GO-PEG-NH_2 was applied as a drug delivery system for paclitaxel (PTX). The cytostatic was attached by non-covalent functionalisation through π–π stacking and hydrophobic interactions (Fig. 13). In

addition to these covalent conjugates, GBN was applied as additives to various nanocomposite materials.

Yu et al. performed the modification of polystyrene (PS) with 2 wt % GO and obtained materials with superior anti-corrosion properties (protection efficiency against corrosion increased from 37.90% to 99.53% in comparison to PS), increased thermal stability (from 73 for PS to 372 °C for GO-PS) and enhanced mechanical properties (the storage modulus increased from 1808.76 MPa for PS to 2802.36 MPa for GO-PS) [164]. Deshmukh et al. carried out the synthesis of a nanocomposite based on polyvinylchloride (PVC) modified with GO (the quantity of GO varied from 0.5 to 2.5 wt %). It was demonstrated that the incorporation of GO to PVC leads to decrease in surface roughness through improving the values of contact angle [165]. Ovcharenko et al. demonstrated that GO-poly(carbonate-urea)urethane nanocomposite can be applied in the development of artificial heart valves due to its superior mechanical properties, hemocompatibility, and calcific resistance of nanocomposites [166]. Kumar et al. revealed that the nanocomposite based on sulfonated GO and sulfonated polyether ether ketone (SGO-SPEEK) demonstrated high proton conductivity of 0.055 S cm $^{-1}$ at 80^{0}C and 30% RH compared to the non-modified SPEEK (0.015 S cm $^{-1}$). Thus, the obtained nanomaterial can be used for the development of fuel cells [167].

2.4 Graphene conjugation with anticancer drugs

Literature shows that GBN was conjugated with anticancer drugs through noncovalent interaction of the drug with graphene surface. Zhang et al. [168] reported that covalent functionalisation of GO with sulfonic acid groups and folic acid (GO-SO_3H-FA) allowed to increase the specificity towards MCF-7 cells (human breast cancer cell line). Addition of anticancer drugs (doxorubicine (DOX) and camptothecin (CPT)) through non-covalent

functionalisation (due to π–π stacking and hydrophobic interactions between the drugs and the GO surface) significantly increase the therapeutic efficacy in comparison with individual drugs. The amount of CPT and DOX on GO-SO_3H-FA-CPT-DOX was calculated to be 4.5 % and 400% respectively.

Wang et al. [104] demonstrated that the covalent functionalisation of GO with chlorotoxin (CTX) increases the drug delivery to C6 glioma cells. At the same time, non-covalent attachment of DOX with the capacity of 570 mg DOX per gram CTX-GO significantly increases the efficiency of the conjugate (the release of the drug was pH dependent). Fan et al. [169] synthesised covalent conjugate based on GO with adipic acid dihydrazide and sodium alginate (SA). Then, DOX·HCl was non-covalently attached to GO-SA, the maximum capacity of DOX on GO–SA was 1.8 mg/mg GO-SA with the best drug release rate at pH 5.0. The cytotoxicity measurements demonstrated that GO–SA conjugate did not bear toxicity while GO–SA/DOX showed cytotoxicity towards HeLa (human cervical carcinoma cell line) through specific targeting of CD44 receptors.

Qin et al. [170] prepared GO non-covalently conjugated with polyvinylpyrrolidone (PVP, M= 30 kDa) and then folic acid (FA) was covalently attached to COOH groups of GO through amide bond formation followed by the non-covalent attachment of DOX to the surface of FA–GO–PVP (through π–π stacking and hydrophobic interactions). The load ratio of DOX on FA–GO–PVP was calculated to be 107.5 wt%. The obtained conjugate demonstrated high anticancer efficacy on HeLa cells. Huang et al. [171] described the ability of GO functionalised with FA to efficiently load chlorin e6 photosensitiser for targeted photodynamic therapy. Tiwari et al. [172] used GO-PVP non-covalent conjugate for the dual non-covalent attachment of quercetin (QS) and gefitinib (GF) and compared it with the GO-PVP-QS and GO-PVP-GF conjugates. The

authors found that the combined drug loading had high cytotoxicity against PA-1 cells (ovarian cancer cell line) compared with the individual drugs and the free drugs. The amount of QS and GF in GO-PVP-QS-GF was equal to 20 and 46% respectively.

GO was functionalised with polyethylene glycol, FA, and CPT by non-covalent π–π stacking interactions (CPT percentage was 45%) and achieved 76% cytotoxicity towards MCF-7 (breast cancer cell line) at the highest applied concentration (100 $\mu g \cdot ml^{-1}$) [173]. In addition, magnetic GO surface was grafted by β-cyclodextrin (β-CD, M=1.1 kDa) for the delivery of DOX and methotrexate (MTX). The cytotoxicity results on K562 cells (leukemia cell line) showed decreasing cell viability by 65% and 55% at the concentration of 16 $\mu g \cdot ml^{-1}$ for GO-Fe_3O_4-β-CD-DOX (37.4% of DOX) and GO-Fe_3O_4-β-CD-MTX (23.4 % of MTX), respectively [174].

GO was functionalised with natural polymer chitosan (CS) and FA for the delivery of CPT and 3,3′-diindolylmethane (DIM). The obtained conjugate (GO-CS-FA-CPT-DIM) demonstrated increased cytotoxicity against MCF-7 cell line using MTT assay (95.67 % decrease of the cell viability) that was significantly higher in comparison with the pure drugs DIM (42.4 %) and CPT (52.59 %) [175]. Pei et al. revealed that the simultaneous attachment of Pt and DOX to GO surface functionalized with PEG (pGO) (pGO-Pt-DOX, weight ratio: 1:0.376:0.376) leads to enhanced cytotoxicity against both Cal-27 (human squamous cell carcinoma cell line) and MCF-7 (breast cancer cell line). The authors observed a higher inhibition rate for the pGO-CP-DOX conjugate in comparison with individual drugs: IC_{50} (MCF-7) =14.5 $\mu g \cdot ml^{-1}$ for pGO-Pt-DOX, 22.5 $\mu g \cdot ml^{-1}$ for pGO-DOX and 22 $\mu g \cdot ml^{-1}$ for pGO-CP [176]. Bullo et al. demonstrated the possibility of GO functionalisation with PEG, FA, and anticancer drugs protocatechuic acid (23.47% PCA) and chlorogenic acid (18.33% CA-). The authors studied the conjugate GO-PEG-FA-PCA-CA against two cancer cells HT29 (colon cancer cells) and HePG2 (human liver cancer

cells). Cytotoxicity experiments revealed the following results: IC_{50} (HT29) = 50.69 μg·ml^{-1}, IC_{50} (HepG2) = 40.39 μg·ml^{-1}[177]. Gong et al. demonstrated that fluorinated graphene (FG) was used to load the mixture of DOX and CPT after covalent functionalisation with CS; the load of DOX and CPT was equal to 110% and 25%, respectively. The obtained conjugate FG-CS-DOX-CPT demonstrated the decrease of cell viability towards HeLa cell line by 60 and 75% under laser irradiation at 808 nm [178]. Gong et al. in another study showed the possibility of carrying out non-covalent conjugation of FG with DOX (at 200%). FG-DOX conjugate at the concentration of 30 μg·ml^{-1} significantly decreased the cell viability of HeLa cancer cell line up to 94 % after 48 h incubation [179].

Shim et al. revealed in *in-vivo* study that rGO functionalised with low-molecular-weight heparin (LHT7) acted as a tumor-targeting molecule for the delivery of DOX. The conjugate rGO-LHT7-DOX with rGO:DOX weight ratios 2, 1, 0.5, 0.1, demonstrated high anti-tumor effect against human KB carcinoma cells (61.1 % decrease of cell viability) as well as significant reducing of tumor size by (92.5 ± 3.1)% [180]. Table 3 summarises examples of conjugation between anticancer drugs and the surface of GBN.

2.5 Graphene conjugations with biomolecules

Graphene and GO were conjugated with short chain peptides, enzymes, and proteins by covalent or non-covalent attachment. These molecules can react with the surface of graphene or the various oxygen functional groups of GO (carboyxyl, hydroxyl, epoxy, and carbonyl groups), for example by forming amide bond between the carboxylic group of GO and the NH_2 group of the enzyme or the protein. Also, the non-covalent attachment can take place through hydrophobic, electrostatic, or π–π interactions [181,182].

Wang et al. [183] showed the possibility of covalent conjugation of GO with antibodies (Ab) using bifunctional PEG (NH_2–PEG–COOH) as a linker. The carboxylic groups of GO linked with the amino groups of PEG by EDC coupling forming amide bonds and then the COOH groups of PEG were coupled with NH_2 groups of the antibody forming GO-PEG-Ab by the same reaction. The obtained material can be used as sensors with high sensitivity towards small molecules as antigens. Jokar et al. [184] performed covalent functionalisation of GO with polyethylene glycol (M = 1 KDa) and HSA with subsequent non-covalent π–π interactions with PTX for drug delivery (the PTX-loading was equal to 22%). The authors pointed out that the release rate of PTX was faster in the acidic mediums (at pH values of 5 and 6.8).

Kim et al. [185] showed that GO can be covalently conjugated with polyethylenimine (M= 1.8 kDa) as a gene delivery cationic vector through π–π stacking interactions with GO surface. At the same time, the conjugate acted as a bioimaging material due to its excellent photoluminescence properties. In our group GO was covalently functionalised with L-methionine [186] and L-cysteine [187] through amidation reaction. Moreover, we demonstrated the high biocompatibility of these materials, in particular hemocompatibility without cyto- or genotoxicity.

The authors of [188–190] performed covalent and non-covalent conjugation of GBN with biomolecules such as DNA, peptides, proteins, enzymes, carbohydrates, and viruses for various applications, for example, drug delivery, cancer treatment, tissue engineering, bioimaging as well as the development of biosensors for detecting very low concentrations of biomolecules such as antibodies, nucleic acids, enzymes, or proteins especially for early diagnosis of diseases [191–196]. Wang et al. [193] demonstrated that graphene covalently modified by antibodies can detect in earlier stages the disease markers such as hormones, enzymes, proteins, sugars, peptides, and

disease related genes. Zhang et al. [181] demonstrated that GO covalently and non-covalently linked with proteins (as BSA and trypsin), enzymes and peptides, can be applied as a platform for further immobilisation of Au nanoparticles for the application to biosensors and synthesising novel graphene-based nanoarchitectures. Lu et al. [197] performed the covalent functionalisation of amino-modified DNA with GO through amidation reaction using EDC coupling for the purpose of detecting heavy metals.

3. Biocompatibility of GBN

Biocompatibility investigations of new materials usually include the study of haemolysis, thrombocyte aggregation, binding to human serum albumin (HSA), genotoxicity, cytotoxicity, and plasma-coagulation haemostasis.

3.1 Haemolysis

Literature analysis reveals that the functionalisation of graphene surface leads to decreasing the haemolysis and thus increasing haemocompatibility. Liao et al. [198] showed that GO has dose dependent hemolytic activity with TC_{50} = 20.2-49.6 μg·ml^{-1} which is the concentration of GO that causes 50% haemolysis, while graphene sheets showed insignificant hemolysis (TC_{50} > 200 μg·ml^{-1}). At the same time, the noncovalent functionalisation of GO with chitosan didn't demonstrate any hemolytic activity pointing out that the functionalisation can protect erythrocytes. Pinto et al. [199] showed that the noncovalent functionalisation of graphene surface by polymers (poly(vinyl alcohol), poly(ethylene glycol), poly(vinyl pyrrolidone), hydroxyethyl cellulose, chondroitin, glucosamine, and hyaluronic acid resulted in decreasing haemolysis to less than 1.7 % for all materials at concentrations up to 500 μg·ml^{-1}. In our previous works GO enriched by oxygen containing groups (EOGO) as well as GO functionalised

with L-methionine (GFM) and L-cysteine (GFC) did not cause erythrocyte membrane damage at up to 25 μg·ml^{-1} [98,186,200].

3.2 Thrombocyte aggregation

Singh et al. [201,202] demonstrated that GO (C = 2 μg·ml^{-1}) induced platelet aggregation. The functionalisation of GO with amine functional groups did not activate platelet aggregation at the same concentration range. The authors showed that the aggregation caused by GO was even stronger than that initiated by thrombin. Podolska et al. [203] determined that GO, rGO, and rGO-PEG (C= 50 μg·ml^{-1}) did not stimulate platelet aggregation in the presence of 2 μmol·ml^{-1} of adenosine diphosphate (ADP). GFC (up to 25 μg·l^{-1}) did not stimulate the ADP-induced aggregation of platelets while GFM and EOGO demonstrated anti-aggregation activity up to 25 μg·l^{-1} and 100 μg·l^{-1} respectively, in the experiments of ADP and collagen induced aggregation.

3.3 Binding to human serum albumin

Ding et al. [204] revealed that GO (100 μg ml^{-1}) can interact with HSA through various types of interactions (covalent bonds, hydrogen bonds, electrostatic forces, hydrophobic and π–π stacking interactions). The interaction between GO and HSA led to malfunctioning of HSA and its inability to remove toxins due to conformational changes, meaning that GO is potentially toxic. The functionalisation of GO surface by carboxylic groups (GO-COOH, 100 μg ml^{-1}) showed increasing biocompatibility as it didn't cause functional changes of HSA. In contrast, Taneva et al. [205] demonstrated that GO (8 mg ml^{-1}) interaction with HSA did not cause toxic effect for HSA in the blood plasma due to the low affinity of GO to HSA.

Ding et al. [204] determined the values of the dissociation constant (the reciprocal of the binding constant) of the HSA complex with GO (K_d= 27.5 μg·ml^{-1}). The authors proposed that the formation of covalent bonds is due to the interaction of GO epoxy groups and free amino

groups of Lys and Arg of HSA by the nucleophilic addition mechanism and hydrogen bonding. In turn, the interaction of modified GO with HSA mainly occurs due to the formation of hydrogen bonds because the epoxy groups are blocked by the carboxyl groups: the dissociation constant value for the interaction between GFM, GFC, and HSA are equal to 185.2 [186] and 1600 [98] $\mu g \cdot ml^{-1}$, respectively.

3.4 Genotoxicity

Liu at al. [206] revealed that GO at concentrations up to 100 $\mu g\ ml^{-1}$ induced mutagenesis due to interfering with DNA replication and altering gene expression patterns. Wang et al. [207] reported that GO (up to 100 $\mu g\ ml^{-1}$) possessed significant genotoxicity to human lung fibroblast (HLF) cells due to DNA damage through the generation of reactive oxygen species and surface charge of GO. After functionalisation of GO surface with PEG and lactobionic acid, the genotoxicity was significantly decreased.

Akhavan et al. [208] demonstrated that the genotoxicity is dependent on lateral size dimensions of graphene: the rGO nanoparticles with average lateral dimensions of 11±4 nm were able to penetrate into the nucleus of the human mesenchymal stem cells (hMSCs) leading to DNA fragmentations and chromosomal aberrations at low concentrations (0.1 and 1.0 $mg \cdot ml^{-1}$) after 1 h. At the same time rGO sheets with average lateral dimensions of 3.8±0.4 μm did not exhibit genotoxicity even at 100 $mg \cdot ml^{-1}$ after 24 h. Both GFM and GFC did not demonstrate genotoxicity up to 25 $\mu g \cdot ml^{-1}$ as well as less genotoxicity recorded for EOGO up to the concentrations of 100 $\mu g\ ml^{-1}$[209].

3.5 Cytotoxicity

Wang et al. [210] indicated that GO (10-200 $\mu g\ ml^{-1}$) cause cytotoxicity in a dose dependent manner to human multiple myeloma RPMI 8226 cells through oxidative stress mechanism.

Akhavan et al. [208] revealed that the cytotoxicity of graphene is size and concentration dependent. rGO with average lateral dimension 11 ±4 nm is cytotoxic to hMSCs at 1 μg ml^{-1} while rGO with larger average lateral dimension of 3.8 ± 0.4 μm showed less cytotoxicity at higher concentration of 100 μg ml^{-1}. Sun et al. [211] showed that the functionalisation of graphene surface with hydroxyl functional groups (G-OH) preserves viability of rat adipose tissue-derived stromal cells (rADSCs). Wu et al. [212] demonstrated that covalently functionalised GO with adipic acid dihydrazide (AD) and hyaluronic acid (HA) had no cytotoxic effect towards HeLa and L929 cell lines up to 200 μg·ml^{-1}. In addition, GFM, GFC, and EOGO did not demonstrate cytotoxicity towards HEK293 cell line up to 25 mg·l^{-1}.[98,186,209]

4. GBN dispersion stability

It is well known that graphene, GO, and rGO have different stability of colloid dispersions in water. Si et al. demonstrated that pristine graphene has no despersibility because it has no oxygen functional groups and due to having high density of hydrophobic sp^2 C=C bonds [213]. The ability of GBN to form stable dispersions in water is referred to (*i*) the high polarity and forming hydrogen bonds with water [214]; (*ii*) the presence of charged particles leading to high electrostatic repulsion between graphene flakes [215–217].

The importance of GBN dispersions stabilisation is a key point for its biomedical applications. GBN dispersions can be obtained through various approaches: (*i)* exfoliation of graphene in definite solvents without functionalisation or addition of stabilising agents (surfactants or polymers); *(ii)* covalent or noncovalent functionalisation of graphene surface which support stability of aqueous dispersions; *(iii)* using dispersing agents such as surfactants and polymers that can be adsorbed on graphene surface and increase the exfoliation, solvation

and stabilisation of graphene layers in aqueous dispersions [218]. Table 4 demonstrates the characteristics of GBN dispertions.

5. Conclusion

GBN in the form of graphene, GO, and rGO are perspective nanostructures in which the surface is enriched by electrons and various oxygen-containing functional groups are present that allow to perform covalent and non-covalent functionalisation leading to various nanomaterials that are promising in applications in nanobiomedicine (Fig. 14) as targeted drug delivey, the treatment of cancer, tissue engineering, bioimaging, biosensors, developing antimicrobial and antiviral materials as well as in energy applications (batteries, solar cells, fuel cells, superconductors), textiles, and electronics. Among GBN, GO is a leading nanomaterial due to the presence of oxygen-containing functional groups along with the π structure that can be exploited as a nanoplatform for covalent or non-covalent loading of organic and inorganic compounds. At the same time the presence of the functional groups provides the stability of GO aqueous dispersions in contrast to graphene or rGO.

6. Future remarks/recommendations

This review summarises the results of studies on covalent and noncovalent functionalisation of graphene surface. Particular attention is paid to establishing the relationship between the type of functionalisation and the possibilities of GBN application in various fields of science and technology. Literature analysis reveals the following trends in the study of GBN:

(*i*) there is a large body of data on covalent and noncovalent modification of graphene surface which allows to vary the physicochemical properties of the final nanomaterial and affect the GBN dispersions stability;

(*ii*) large number of scientific works are devoted to the application of GBN as nanomodifiers. The implementation of this approach makes it possible to obtain new materials with unique physicochemical and operational characteristics;

(*iii*) extremely relevant direction is devoted to the application of GBN in medicine and bioanalysis. In this regard, the number of publications on the study of biocompatibility, as well as *in vitro* and *in vivo* studies of GBN is increasing annually.

At the same time, detailed analysis of the literature data reveals the following drawbacks and problems that deserve special attention:

(*i*) lack of data on identification of the synthesised nanomaterial. Often, the authors do not conduct a comprehensive study of the structure and composition of the obtained materials;

(*ii*) the question of reproducibility of GBN syntheses remains open;

(*iii*) the literature presents a small number of studies aimed at studying the stability of GBN dispertions;

(*iv*) there is no data on the metabolic pathways and toxicokinetics of GBN for biomedicinal purposes;

(*v*) GBN biomedicinal studies are not comprehensive and do not allow to analyse the full profile of the possibilities of using these nanomaterials.

Acknowledgements

The work was supported by the Council on Grants of the President of the Russian Federation for State Support of Young Scientists (MD-741.2020.7). The research of Abdelsattar Osama Elemam Abdelhalim is funded by the scholarship EGY-6218/17 under the Joint Executive Program between the Arab Republic of Egypt and the Russian Federation. The equipment of the following Resource Centres of the Research Park of Saint Petersburg State University was used: Resource Centre “GeoModel”, the Centre for Diagnostics of Functional Materials for Medicine, Pharmacology and Nanoelectronics, Interdisciplinary Resource Centre for Nanotechnology, Magnetic Resonance Research Centre, Centre for Physical Methods of Surface Investigation, Centre for Chemical Analysis and Materials Research, Thermogravimetric and Calorimetric Research Centre.

References

[1] S.R. Shin, Y.C. Li, H.L. Jang, P. Khoshakhlagh, M. Akbari, A. Nasajpour, Y.S. Zhang, A. Tamayol, A. Khademhosseini, Graphene-based materials for tissue engineering, Adv. Drug Deliv. Rev. 105 (2016) 255–274. https://doi.org/10.1016/j.addr.2016.03.007.

[2] J. Lin, Y. Huang, P. Huang, Graphene-Based Nanomaterials in Bioimaging, in: Biomed. Appl. Funct. Nanomater. Concepts, Dev. Clin. Transl., Elsevier, 2018: pp. 247–287. https://doi.org/10.1016/B978-0-323-50878-0.00009-4.

[3] L.L. Feng, Y.X. Wu, D.L. Zhang, X.X. Hu, J. Zhang, P. Wang, Z.L. Song, X.B. Zhang, W. Tan, Near Infrared Graphene Quantum Dots-Based Two-Photon Nanoprobe for Direct Bioimaging of Endogenous Ascorbic Acid in Living Cells, Anal. Chem. 89 (2017) 4077–4084. https://doi.org/10.1021/acs.analchem.6b04943.

[4] H. yang Fan, X. hua Yu, K. Wang, Y. jia Yin, Y. jie Tang, Y. ling Tang, X. hua Liang, Graphene quantum dots (GQDs)-based nanomaterials for improving photodynamic therapy in cancer treatment, Eur. J. Med. Chem. 182 (2019) 111620. https://doi.org/10.1016/j.ejmech.2019.111620.

[5] R.K. Thapa, J.H. Kim, J.H. Jeong, B.S. Shin, H.G. Choi, C.S. Yong, J.O. Kim, Silver nanoparticle-embedded graphene oxide-methotrexate for targeted cancer treatment, Colloids Surfaces B Biointerfaces. 153 (2017) 95–103. https://doi.org/10.1016/j.colsurfb.2017.02.012.

[6] C. Zhang, Z. Liu, Y. Zheng, Y. Geng, C. Han, Y. Shi, H. Sun, C. Zhang, Y. Chen, L. Zhang, Q. Guo, L. Yang, X. Zhou, L. Kong, Glycyrrhetinic Acid Functionalized Graphene Oxide for Mitochondria Targeting and Cancer Treatment In Vivo, Small. 14 (2018) 1703306. https://doi.org/10.1002/smll.201703306.

[7] J. Liu, J. Dong, T. Zhang, Q. Peng, Graphene-based nanomaterials and their potentials in advanced drug delivery and cancer therapy, J. Control. Release. 286 (2018) 64–73. https://doi.org/10.1016/j.jconrel.2018.07.034.

[8] D. Iannazzo, A. Pistone, M. Salamò, S. Galvagno, R. Romeo, S. V. Giofré, C. Branca, G. Visalli, A. Di Pietro, Graphene quantum dots for cancer targeted drug delivery, Int. J. Pharm. 518 (2017) 185–192. https://doi.org/10.1016/j.ijpharm.2016.12.060.

[9] K. Yang, L. Feng, Z. Liu, Stimuli responsive drug delivery systems based on nano-graphene for cancer therapy, Adv. Drug Deliv. Rev. 105 (2016) 228–241. https://doi.org/10.1016/j.addr.2016.05.015.

[10] X. Hai, J. Feng, X. Chen, J. Wang, Tuning the optical properties of graphene quantum dots for biosensing and bioimaging, J. Mater. Chem. B. 6 (2018) 3219–3234. https://doi.org/10.1039/c8tb00428e.

[11] S. Szunerits, R. Boukherroub, Graphene-based biosensors, Interface Focus. 8 (2018) 20160132. https://doi.org/10.1098/rsfs.2016.0132.

[12] J. Peña-Bahamonde, H.N. Nguyen, S.K. Fanourakis, D.F. Rodrigues, Recent advances in graphene-based biosensor technology with applications in life sciences, J. Nanobiotechnology. 16 (2018) 1–17. https://doi.org/10.1186/s12951-018-0400-z.

[13] V. Palmieri, M. Papi, Can graphene take part in the fight against COVID-19?, Nano Today. 33 (2020) 100883. https://doi.org/10.1016/j.nantod.2020.100883.

[14] X.X. Yang, C.M. Li, Y.F. Li, J. Wang, C.Z. Huang, Synergistic antiviral effect of curcumin functionalized graphene oxide against respiratory syncytial virus infection, Nanoscale. 9 (2017) 16086–16092. https://doi.org/10.1039/c7nr06520e.

[15] Y.-N. Chen, Y.-H. Hsueh, C.-T. Hsieh, D.-Y. Tzou, P.-L. Chang, Antiviral Activity of

Graphene–Silver Nanocomposites against Non-Enveloped and Enveloped Viruses, Int. J. Environ. Res. Public Health. 13 (2016) 430. https://doi.org/10.3390/ijerph13040430.

[16] T. Du, J. Lu, L. Liu, N. Dong, L. Fang, S. Xiao, H. Han, Antiviral Activity of Graphene Oxide-Silver Nanocomposites by Preventing Viral Entry and Activation of the Antiviral Innate Immune Response, ACS Appl. Bio Mater. 1 (2018) 1286–1293. https://doi.org/10.1021/acsabm.8b00154.

[17] L. Shi, J. Chen, L. Teng, L. Wang, G. Zhu, S. Liu, Z. Luo, X. Shi, Y. Wang, L. Ren, The Antibacterial Applications of Graphene and Its Derivatives, Small. 12 (2016) 4165–4184. https://doi.org/10.1002/smll.201601841.

[18] H. Ji, H. Sun, X. Qu, Antibacterial applications of graphene-based nanomaterials: Recent achievements and challenges, Adv. Drug Deliv. Rev. 105 (2016) 176–189. https://doi.org/10.1016/j.addr.2016.04.009.

[19] M.Y. Xia, Y. Xie, C.H. Yu, G.Y. Chen, Y.H. Li, T. Zhang, Q. Peng, Graphene-based nanomaterials: the promising active agents for antibiotics-independent antibacterial applications, J. Control. Release. 307 (2019) 16–31. https://doi.org/10.1016/j.jconrel.2019.06.011.

[20] P. Kumar, P. Huo, R. Zhang, B. Liu, Antibacterial Properties of Graphene-Based Nanomaterials, Nanomaterials. 9 (2019) 737. https://doi.org/10.3390/nano9050737.

[21] X. Wu, H. Li, N. Xiao, Advancement of Near-infrared (NIR) laser interceded surface enactment of proline functionalized graphene oxide with silver nanoparticles for proficient antibacterial, antifungal and wound recuperating therapy in nursing care in hospitals, J. Photochem. Photobiol. B Biol. 187 (2018) 89–95. https://doi.org/10.1016/j.jphotobiol.2018.07.015.

[22] M.H. Kahsay, N. Belachew, A. Tadesse, K. Basavaiah, Magnetite nanoparticle decorated reduced graphene oxide for adsorptive removal of crystal violet and antifungal activities, RSC Adv. 10 (2020) 34916–34927. https://doi.org/10.1039/d0ra07061k.

[23] J. Zhang, J. Zhang, F. Zhang, H. Yang, X. Huang, H. Liu, S. Guo, Graphene oxide as a matrix for enzyme immobilization, Langmuir. 26 (2010) 6083–6085. https://doi.org/10.1021/la904014z.

[24] S. Hermanová, M. Zarevúcká, D. Bouša, M. Pumera, Z. Sofer, Graphene oxide immobilized enzymes show high thermal and solvent stability, Nanoscale. 7 (2015) 5852–5858. https://doi.org/10.1039/c5nr00438a.

[25] H. Li, K. Fierens, Z. Zhang, N. Vanparijs, M.J. Schuijs, K. Van Steendam, N. Feiner Gracia, R. De Rycke, T. De Beer, A. De Beuckelaer, S. De Koker, D. Deforce, L. Albertazzi, J. Grooten, B.N. Lambrecht, B.G. De Geest, Spontaneous Protein Adsorption on Graphene Oxide Nanosheets Allowing Efficient Intracellular Vaccine Protein Delivery, ACS Appl. Mater. Interfaces. 8 (2016) 1147–1155. https://doi.org/10.1021/acsami.5b08963.

[26] T. Kavitha, I.K. Kang, S.Y. Park, Poly(acrylic acid)-grafted graphene oxide as an intracellular protein carrier, Langmuir. 30 (2014) 402–409. https://doi.org/10.1021/la404337d.

[27] F. Emadi, A. Amini, A. Gholami, Y.G.-S. reports, undefined 2017, Functionalized graphene oxide with chitosan for protein nanocarriers to protect against enzymatic cleavage and retain collagenase activity, Nature.Com. (n.d.).

[28] H. Zhao, R. Ding, X. Zhao, Y. Li, L. Qu, H. Pei, L. Yildirimer, Z. Wu, W. Zhang, Graphene-based nanomaterials for drug and/or gene delivery, bioimaging, and tissue

engineering, Drug Discov. Today. 22 (2017) 1302–1317. https://doi.org/10.1016/j.drudis.2017.04.002.

[29] A. Paul, A. Hasan, H. Al Kindi, A.K. Gaharwar, V.T.S. Rao, M. Nikkhah, S.R. Shin, D. Krafft, M.R. Dokmeci, D. Shum-Tim, A. Khademhosseini, Injectable graphene oxide/hydrogel-based angiogenic gene delivery system for vasculogenesis and cardiac repair, ACS Nano. 8 (2014) 8050–8062. https://doi.org/10.1021/nn5020787.

[30] B. Chen, M. Liu, L. Zhang, J. Huang, J. Yao, Z. Zhang, Polyethylenimine-functionalized graphene oxide as an efficient gene delivery vector, J. Mater. Chem. 21 (2011) 7736–7741. https://doi.org/10.1039/c1jm10341e.

[31] R. Imani, W. Shao, S. Taherkhani, S.H. Emami, S. Prakash, S. Faghihi, Dual-functionalized graphene oxide for enhanced siRNA delivery to breast cancer cells, Colloids Surfaces B Biointerfaces. 147 (2016) 315–325. https://doi.org/10.1016/j.colsurfb.2016.08.015.

[32] H. Yue, X. Zhou, M. Cheng, D. Xing, Graphene oxide-mediated Cas9/sgRNA delivery for efficient genome editing, Nanoscale. 10 (2018) 1063–1071. https://doi.org/10.1039/c7nr07999k.

[33] Z. Tang, H. Wu, J.R. Cort, G.W. Buchko, Y. Zhang, Y. Shao, I.A. Aksay, J. Liu, Y. Lin, Constraint of DNA on functionalized graphene improves its biostability and specificity, Small. 6 (2010) 1205–1209. https://doi.org/10.1002/smll.201000024.

[34] C.H. Lu, C.L. Zhu, J. Li, J.J. Liu, X. Chen, H.H. Yang, Using graphene to protect DNA from cleavage during cellular delivery, Chem. Commun. 46 (2010) 3116–3118. https://doi.org/10.1039/b926893f.

[35] U.R. Farooqui, A.L. Ahmad, N.A. Hamid, Graphene oxide: A promising membrane

material for fuel cells, Renew. Sustain. Energy Rev. 82 (2018) 714–733. https://doi.org/10.1016/j.rser.2017.09.081.

[36] J. Liu, H.J. Choi, L.Y. Meng, A review of approaches for the design of high-performance metal/graphene electrocatalysts for fuel cell applications, J. Ind. Eng. Chem. 64 (2018) 1–15. https://doi.org/10.1016/j.jiec.2018.02.021.

[37] R. Kumar, S. Sahoo, E. Joanni, R.K. Singh, W.K. Tan, K.K. Kar, A. Matsuda, Recent progress in the synthesis of graphene and derived materials for next generation electrodes of high performance lithium ion batteries, Prog. Energy Combust. Sci. 75 (2019) 100786. https://doi.org/10.1016/j.pecs.2019.100786.

[38] Y. Zhang, X. Xia, B. Liu, S. Deng, D. Xie, Q. Liu, Y. Wang, J. Wu, X. Wang, J. Tu, Multiscale Graphene-Based Materials for Applications in Sodium Ion Batteries, Adv. Energy Mater. 9 (2019). https://doi.org/10.1002/aenm.201803342.

[39] T. Mahmoudi, Y. Wang, Y.B. Hahn, Graphene and its derivatives for solar cells application, Nano Energy. 47 (2018) 51–65. https://doi.org/10.1016/j.nanoen.2018.02.047.

[40] H. Chen, Q. Luo, T. Liu, M. Tai, J. Lin, V. Murugadoss, H. Lin, J. Wang, Z. Guo, N. Wang, Boosting Multiple Interfaces by Co-Doped Graphene Quantum Dots for High Efficiency and Durability Perovskite Solar Cells, ACS Appl. Mater. Interfaces. 12 (2020) 13941–13949. https://doi.org/10.1021/acsami.9b23255.

[41] S. Afroj, N. Karim, Z. Wang, S. Tan, P. He, M. Holwill, D. Ghazaryan, A. Fernando, K.S. Novoselov, Engineering Graphene Flakes for Wearable Textile Sensors via Highly Scalable and Ultrafast Yarn Dyeing Technique, ACS Nano. 13 (2019) 3847–3857. https://doi.org/10.1021/acsnano.9b00319.

[42] S. Hamze, D. Cabaleiro, P. Estellé, Graphene-based nanofluids: A comprehensive review

about rheological behavior and dynamic viscosity, J. Mol. Liq. 325 (2021) 115207. https://doi.org/10.1016/J.MOLLIQ.2020.115207.

[43] S. Hamze, D. Cabaleiro, T. Maré, B. Vigolo, P. Estellé, Shear flow behavior and dynamic viscosity of few-layer graphene nanofluids based on propylene glycol-water mixture, J. Mol. Liq. 316 (2020) 113875. https://doi.org/10.1016/J.MOLLIQ.2020.113875.

[44] D. Cabaleiro, P. Estellé, H. Navas, A. Desforges, B. Vigolo, Dynamic viscosity and surface tension of stable graphene oxide and reduced graphene oxide aqueous nanofluids, J. Nanofluids. 7 (2018) 1081–1088. https://doi.org/10.1166/JON.2018.1539.

[45] A.O.E. Abdelhalim, A. Galal, M.Z. Hussein, I.E.-T. El Sayed, Graphene Functionalization by 1,6-Diaminohexane and Silver Nanoparticles for Water Disinfection, J. Nanomater. 2016 (2016). https://doi.org/10.1155/2016/1485280.

[46] B. Song, C. Zhang, G. Zeng, J. Gong, Y. Chang, Y. Jiang, Antibacterial properties and mechanism of graphene oxide-silver nanocomposites as bactericidal agents for water disinfection, Arch. Biochem. Biophys. 604 (2016) 167–176. https://doi.org/10.1016/j.abb.2016.04.018.

[47] S. Homaeigohar, M. Elbahri, Graphene membranes for water desalination, NPG Asia Mater. 9 (2017) e427–e427. https://doi.org/10.1038/am.2017.135.

[48] J.E. Johns, M.C. Hersam, Atomic covalent functionalization of graphene, Acc. Chem. Res. 46 (2013) 77–86. https://doi.org/10.1021/ar300143e.

[49] J.M. Englert, C. Dotzer, G. Yang, M. Schmid, C. Papp, J.M. Gottfried, H.P. Steinrück, E. Spiecker, F. Hauke, A. Hirsch, Covalent bulk functionalization of graphene, Nat. Chem. 3 (2011) 279–286. https://doi.org/10.1038/nchem.1010.

[50] J. Park, M. Yan, Covalent functionalization of graphene with reactive intermediates, Acc.

Chem. Res. 46 (2013) 181–189. https://doi.org/10.1021/ar300172h.

[51] A. Criado, M. Melchionna, S. Marchesan, M. Prato, The Covalent Functionalization of Graphene on Substrates, Angew. Chemie - Int. Ed. 54 (2015) 10734–10750. https://doi.org/10.1002/anie.201501473.

[52] K.S. Subrahmanyam, A. Ghosh, A. Gomathi, A. Govindaraj, C.N.R. Rao, Covalent and Noncovalent Functionalization and Solubilization of Graphene, Nanosci. Nanotechnol. Lett. 1 (2011) 28–31. https://doi.org/10.1166/nnl.2009.1014.

[53] H. Bai, Y. Xu, L. Zhao, C. Li, G. Shi, Non-covalent functionalization of graphene sheets by sulfonated polyaniline, Chem. Commun. (2009) 1667–1669. https://doi.org/10.1039/b821805f.

[54] A. Ghosh, K.V. Rao, S.J. George, C.N.R. Rao, Noncovalent functionalization, exfoliation, and solubilization of graphene in water by employing a fluorescent coronene carboxylate, Chem. - A Eur. J. 16 (2010) 2700–2704. https://doi.org/10.1002/chem.200902828.

[55] V. Georgakilas, J.N. Tiwari, K.C. Kemp, J.A. Perman, A.B. Bourlinos, K.S. Kim, R. Zboril, Noncovalent Functionalization of Graphene and Graphene Oxide for Energy Materials, Biosensing, Catalytic, and Biomedical Applications, Chem. Rev. 116 (2016) 5464–5519. https://doi.org/10.1021/acs.chemrev.5b00620.

[56] J.A. Mann, J. Rodríguez-López, H.D. Abruña, W.R. Dichtel, Multivalent binding motifs for the noncovalent functionalization of graphene, J. Am. Chem. Soc. 133 (2011) 17614–17617. https://doi.org/10.1021/ja208239v.

[57] V. Georgakilas, M. Otyepka, A.B. Bourlinos, V. Chandra, N. Kim, K.C. Kemp, P. Hobza, R. Zboril, K.S. Kim, Functionalization of graphene: Covalent and non-covalent approaches, derivatives and applications, Chem. Rev. 112 (2012) 6156–6214.

https://doi.org/10.1021/cr3000412.

[58] D. Wei, Y. Liu, Y. Wang, H. Zhang, L. Huang, G. Yu, Synthesis of n-doped graphene by chemical vapor deposition and its electrical properties, Nano Lett. 9 (2009) 1752–1758. https://doi.org/10.1021/nl803279t.

[59] T.S. Sreeprasad, V. Berry, How do the electrical properties of graphene change with its functionalization?, Small. 9 (2013) 341–350. https://doi.org/10.1002/smll.201202196.

[60] L.A. Falkovsky, Optical properties of graphene, J. Phys. Conf. Ser. 129 (2008) 12004. https://doi.org/10.1088/1742-6596/129/1/012004.

[61] B. Qiu, X.W. Zhao, G.C. Hu, W.W. Yue, X.B. Yuan, J.F. Ren, Tuning optical properties of Graphene/WSe2 heterostructure by introducing vacancy: First principles calculations, Phys. E Low-Dimensional Syst. Nanostructures. 116 (2020) 113729. https://doi.org/10.1016/j.physe.2019.113729.

[62] A. Kumar, K. Sharma, A.R. Dixit, A review on the mechanical and thermal properties of graphene and graphene-based polymer nanocomposites: understanding of modelling and MD simulation, Mol. Simul. 46 (2020) 136–154. https://doi.org/10.1080/08927022.2019.1680844.

[63] R. Aradhana, S. Mohanty, S.K. Nayak, Comparison of mechanical, electrical and thermal properties in graphene oxide and reduced graphene oxide filled epoxy nanocomposite adhesives, Polymer (Guildf). 141 (2018) 109–123. https://doi.org/10.1016/j.polymer.2018.03.005.

[64] T. V. Vu, N. V. Hieu, H. V. Phuc, N.N. Hieu, H.D. Bui, M. Idrees, B. Amin, C. V. Nguyen, Graphene/WSeTe van der Waals heterostructure: Controllable electronic properties and Schottky barrier via interlayer coupling and electric field, Appl. Surf. Sci.

507 (2020) 145036. https://doi.org/10.1016/j.apsusc.2019.145036.

[65] Q. Wang, X. Li, L. Wu, P. Lu, Z. Di, Electronic and Interface Properties in Graphene Oxide/Hydrogen-Passivated Ge Heterostructure, Phys. Status Solidi - Rapid Res. Lett. 13 (2019) 1800461. https://doi.org/10.1002/pssr.201800461.

[66] M. Sang, J. Shin, K. Kim, K. Yu, Electronic and Thermal Properties of Graphene and Recent Advances in Graphene Based Electronics Applications, Nanomaterials. 9 (2019) 374. https://doi.org/10.3390/nano9030374.

[67] D.G. Papageorgiou, I.A. Kinloch, R.J. Young, Mechanical properties of graphene and graphene-based nanocomposites, Prog. Mater. Sci. 90 (2017) 75–127. https://doi.org/10.1016/j.pmatsci.2017.07.004.

[68] X. Zhao, Q. Zhang, D. Chen, P. Lu, Enhanced mechanical properties of graphene-based polyvinyl alcohol composites, Macromolecules. 43 (2010) 2357–2363. https://doi.org/10.1021/ma902862u.

[69] H.C. Lee, W.-W. Liu, S.-P. Chai, A.R. Mohamed, C.W. Lai, C.-S. Khe, C.H. Voon, U. Hashim, N.M.S. Hidayah, Synthesis of Single-layer Graphene: A Review of Recent Development, Procedia Chem. 19 (2016) 916–921. https://doi.org/10.1016/j.proche.2016.03.135.

[70] A. Adetayo, D. Runsewe, Synthesis and Fabrication of Graphene and Graphene Oxide: A Review, Open J. Compos. Mater. 09 (2019) 207–229. https://doi.org/10.4236/ojcm.2019.92012.

[71] Y. Zhang, L. Zhang, C. Zhou, Review of chemical vapor deposition of graphene and related applications, Acc. Chem. Res. 46 (2013) 2329–2339. https://doi.org/10.1021/ar300203n.

[72] R. Muñoz, C. Gómez-Aleixandre, Review of CVD synthesis of graphene, Chem. Vap. Depos. 19 (2013) 297–322. https://doi.org/10.1002/cvde.201300051.

[73] X. Li, L. Colombo, R.S. Ruoff, Synthesis of Graphene Films on Copper Foils by Chemical Vapor Deposition, Adv. Mater. 28 (2016) 6247–6252. https://doi.org/10.1002/adma.201504760.

[74] K. Chen, L. Shi, Y. Zhang, Z. Liu, Scalable chemical-vapour-deposition growth of three-dimensional graphene materials towards energy-related applications, Chem. Soc. Rev. 47 (2018) 3018–3036. https://doi.org/10.1039/c7cs00852j.

[75] X. Yang, G. Zhang, J. Prakash, Z. Chen, M. Gauthier, S. Sun, Chemical vapour deposition of graphene: layer control, the transfer process, characterisation, and related applications, Int. Rev. Phys. Chem. 38 (2019) 149–199. https://doi.org/10.1080/0144235X.2019.1634319.

[76] C. Mattevi, H. Kim, M. Chhowalla, A review of chemical vapour deposition of graphene on copper, J. Mater. Chem. 21 (2011) 3324–3334. https://doi.org/10.1039/c0jm02126a.

[77] H. Zhou, W.J. Yu, L. Liu, R. Cheng, Y. Chen, X. Huang, Y. Liu, Y. Wang, Y. Huang, X. Duan, Chemical vapour deposition growth of large single crystals of monolayer and bilayer graphene, Nat. Commun. 4 (2013) 1–8. https://doi.org/10.1038/ncomms3096.

[78] J. Liu, C.K. Poh, D. Zhan, L. Lai, S.H. Lim, L. Wang, X. Liu, N. Gopal Sahoo, C. Li, Z. Shen, J. Lin, Improved synthesis of graphene flakes from the multiple electrochemical exfoliation of graphite rod, Nano Energy. 2 (2013) 377–386. https://doi.org/10.1016/j.nanoen.2012.11.003.

[79] M. Zhou, J. Tang, Q. Cheng, G. Xu, P. Cui, L.C. Qin, Few-layer graphene obtained by electrochemical exfoliation of graphite cathode, Chem. Phys. Lett. 572 (2013) 61–65.

https://doi.org/10.1016/j.cplett.2013.04.013.

[80] P. Yu, S.E. Lowe, G.P. Simon, Y.L. Zhong, Electrochemical exfoliation of graphite and production of functional graphene, Curr. Opin. Colloid Interface Sci. 20 (2015) 329–338. https://doi.org/10.1016/j.cocis.2015.10.007.

[81] K.S. Rao, J. Senthilnathan, Y.F. Liu, M. Yoshimura, Role of peroxide ions in formation of graphene nanosheets by electrochemical exfoliation of graphite, Sci. Rep. 4 (2014) 1–6. https://doi.org/10.1038/srep04237.

[82] H. Wan, C. Wei, K. Zhu, Y. Zhang, C. Gong, J. Guo, J. Zhang, L. Yu, J. Zhang, Preparation of graphene sheets by electrochemical exfoliation of graphite in confined space and their application in transparent conductive films, ACS Appl. Mater. Interfaces. 9 (2017) 34456–34466. https://doi.org/10.1021/acsami.7b09891.

[83] A. Mir, A. Shukla, Bilayer-rich graphene suspension from electrochemical exfoliation of graphite, Mater. Des. 156 (2018) 62–70. https://doi.org/10.1016/j.matdes.2018.06.035.

[84] A. V. Melezhik, V.F. Pershin, N.R. Memetov, A.G. Tkachev, Mechanochemical synthesis of graphene nanoplatelets from expanded graphite compound, Nanotechnologies Russ. 11 (2016) 421–429. https://doi.org/10.1134/S1995078016040121.

[85] L.G. Guex, B. Sacchi, K.F. Peuvot, R.L. Andersson, A.M. Pourrahimi, V. Ström, S. Farris, R.T. Olsson, Experimental review: Chemical reduction of graphene oxide (GO) to reduced graphene oxide (rGO) by aqueous chemistry, Nanoscale. 9 (2017) 9562–9571. https://doi.org/10.1039/c7nr02943h.

[86] K.K.H. De Silva, H.H. Huang, R.K. Joshi, M. Yoshimura, Chemical reduction of graphene oxide using green reductants, Carbon N. Y. 119 (2017) 190–199. https://doi.org/10.1016/j.carbon.2017.04.025.

[87] J. Wang, E.C. Salihi, L. Šiller, Green reduction of graphene oxide using alanine, Mater. Sci. Eng. C. 72 (2017) 1–6. https://doi.org/10.1016/j.msec.2016.11.017.

[88] S.N. Alam, N. Sharma, L. Kumar, Synthesis of Graphene Oxide (GO) by Modified Hummers Method and Its Thermal Reduction to Obtain Reduced Graphene Oxide (rGO)*, Graphene. 06 (2017) 1–18. https://doi.org/10.4236/graphene.2017.61001.

[89] H. Saleem, M. Haneef, H.Y. Abbasi, Synthesis route of reduced graphene oxide via thermal reduction of chemically exfoliated graphene oxide, Mater. Chem. Phys. 204 (2018) 1–7. https://doi.org/10.1016/j.matchemphys.2017.10.020.

[90] A.E.F. Oliveira, G.B. Braga, C.R.T. Tarley, A.C. Pereira, Thermally reduced graphene oxide: synthesis, studies and characterization, J. Mater. Sci. 53 (2018) 12005–12015. https://doi.org/10.1007/s10853-018-2473-3.

[91] A. Schedy, M. Oetken, The thermal reduction of graphene oxide – A simple and exciting manufacturing process of graphene, CHEMKON. 27 (2020) 244–249. https://doi.org/10.1002/ckon.201900049.

[92] A. Kaplan, Z. Yuan, J.D. Benck, A. Govind Rajan, X.S. Chu, Q.H. Wang, M.S. Strano, Current and future directions in electron transfer chemistry of graphene, Chem. Soc. Rev. 46 (2017) 4530–4571. https://doi.org/10.1039/c7cs00181a.

[93] Z. Sun, D.K. James, J.M. Tour, Graphene Chemistry: Synthesis and Manipulation, J. Phys. Chem. Lett. 2 (2011) 2425–2432. https://doi.org/10.1021/jz201000a.

[94] K.P. Loh, Q. Bao, P.K. Ang, J. Yang, The chemistry of graphene, J. Mater. Chem. 20 (2010) 2277–2289. https://doi.org/10.1039/b920539j.

[95] J. Sturala, J. Luxa, M. Pumera, Z. Sofer, Frontispiece: Chemistry of Graphene Derivatives: Synthesis, Applications, and Perspectives, Chem. - A Eur. J. 24 (2018).

https://doi.org/10.1002/chem.201882361.

[96] W. Gao, The chemistry of graphene oxide, in: Graphene Oxide Reduct. Recipes, Spectrosc. Appl., Springer International Publishing, 2015: pp. 61–95. https://doi.org/10.1007/978-3-319-15500-5_3.

[97] S. Eigler, A. Hirsch, Chemistry with graphene and graphene oxide - Challenges for synthetic chemists, Angew. Chemie - Int. Ed. 53 (2014) 7720–7738. https://doi.org/10.1002/anie.201402780.

[98] A.O.E. Abdelhalim, V. V. Sharoyko, A.A. Meshcheriakov, S.D. Martynova, S. V. Ageev, G.O. Iurev, H. Al Mulla, A. V. Petrov, I.L. Solovtsova, L. V. Vasina, I. V. Murin, K.N. Semenov, Reduction and functionalization of graphene oxide with L-cysteine: Synthesis, characterization and biocompatibility, Nanomedicine Nanotechnology, Biol. Med. 29 (2020) 102284. https://doi.org/10.1016/j.nano.2020.102284.

[99] M.P. Lavin-Lopez, A. Paton-Carrero, L. Sanchez-Silva, J.L. Valverde, A. Romero, Influence of the reduction strategy in the synthesis of reduced graphene oxide, Adv. Powder Technol. 28 (2017) 3195–3203. https://doi.org/10.1016/j.apt.2017.09.032.

[100] A.K. Geim, K.S. Novoselov, The rise of graphene, in: Nanosci. Technol. A Collect. Rev. from Nat. Journals, World Scientific Publishing Co., 2009: pp. 11–19. https://doi.org/10.1142/9789814287005_0002.

[101] B.C. Brodie, XIII. On the atomic weight of graphite, Philos. Trans. R. Soc. London. 149 (1859) 249–259.

[102] R.E. Hummers, W.S., Jr., Offeman, Preparation of Graphitic Oxide, J. Am. Chem. Soc. 80 (1958) 1339.

[103] G. Eskiizmir, Y. Baskin, K. Yapici, Graphene-based nanomaterials in cancer treatment

and diagnosis, in: Fullerenes, Graphenes Nanotub. A Pharm. Approach, Elsevier, 2018: pp. 331–374. https://doi.org/10.1016/B978-0-12-813691-1.00009-9.

[104] H. Wang, W. Gu, N. Xiao, L. Ye, Q. Xu, Chlorotoxin-conjugated graphene oxide for targeted delivery of an anticancer drug, Int. J. Nanomedicine. 9 (2014) 1433–1442. https://doi.org/10.2147/IJN.S58783.

[105] H. Kim, R. Namgung, K. Singha, I.K. Oh, W.J. Kim, Graphene oxide-polyethylenimine nanoconstruct as a gene delivery vector and bioimaging tool, Bioconjug. Chem. 22 (2011) 2558–2567. https://doi.org/10.1021/bc200397j.

[106] J. Lee, J. Kim, S. Kim, D.H. Min, Biosensors based on graphene oxide and its biomedical application, Adv. Drug Deliv. Rev. 105 (2016) 275–287. https://doi.org/10.1016/j.addr.2016.06.001.

[107] P. Innocenzi, L. Stagi, Carbon-based antiviral nanomaterials: Graphene, C-dots, and fullerenes. A perspective, Chem. Sci. 11 (2020) 6606–6622. https://doi.org/10.1039/d0sc02658a.

[108] S. Szunerits, R. Boukherroub, Antibacterial activity of graphene-based materials, J. Mater. Chem. B. 4 (2016) 6892–6912. https://doi.org/10.1039/c6tb01647b.

[109] C. Li, X. Wang, F. Chen, C. Zhang, X. Zhi, K. Wang, D. Cui, The antifungal activity of graphene oxide-silver nanocomposites, Biomaterials. 34 (2013) 3882–3890. https://doi.org/10.1016/j.biomaterials.2013.02.001.

[110] M.Z. Hossain, N. Shimizu, In Situ Functionalization of Graphene with Reactive End Group through Amine Diazotization, J. Phys. Chem. C. 121 (2017) 25223–25228. https://doi.org/10.1021/acs.jpcc.7b08454.

[111] M.Z. Hossain, N. Shimizu, Covalent immobilization of gold nanoparticles on graphene, J.

Phys. Chem. C. 123 (2019) 3512–3516. https://doi.org/10.1021/acs.jpcc.8b09619.

[112] X. Wang, W. Xing, P. Zhang, L. Song, H. Yang, Y. Hu, Covalent functionalization of graphene with organosilane and its use as a reinforcement in epoxy composites, Compos. Sci. Technol. 72 (2012) 737–743. https://doi.org/10.1016/j.compscitech.2012.01.027.

[113] M. De Sousa, C.H.Z. Martins, L.S. Franqui, L.C. Fonseca, F.S. Delite, E.M. Lanzoni, D.S.T. Martinez, O.L. Alves, Covalent functionalization of graphene oxide with d-mannose: Evaluating the hemolytic effect and protein corona formation, J. Mater. Chem. B. 6 (2018) 2803–2812. https://doi.org/10.1039/c7tb02997g.

[114] N. Shang, S. Gao, C. Feng, H. Zhang, C. Wang, Z. Wang, Graphene oxide supported N-heterocyclic carbene-palladium as a novel catalyst for the Suzuki-Miyaura reaction, RSC Adv. 3 (2013) 21863–21868. https://doi.org/10.1039/c3ra44620d.

[115] Z. Qian, J. Ma, X. Shan, L. Shao, J. Zhou, J. Chen, H. Feng, Surface functionalization of graphene quantum dots with small organic molecules from photoluminescence modulation to bioimaging applications: An experimental and theoretical investigation, RSC Adv. 3 (2013) 14571–14579. https://doi.org/10.1039/c3ra42066c.

[116] L. Yu, H. Gao, J. Zhao, J. Qiu, C. Yu, Adsorption of aromatic heterocyclic compounds on pristine and defect graphene: A first-principles study, J. Comput. Theor. Nanosci. 8 (2011) 2492–2497. https://doi.org/10.1166/jctn.2011.1985.

[117] H.L. Poh, P. Šimek, Z. Sofer, M. Pumera, Halogenation of graphene with chlorine, bromine, or iodine by exfoliation in a halogen atmosphere, Chem. - A Eur. J. 19 (2013) 2655–2662. https://doi.org/10.1002/chem.201202972.

[118] S. Lai, Y. Jin, X. Sun, J. Pan, W. Du, L. Shi, Aqueous-based bromination of graphene by electrophilic substitution reaction: a defect-free approach for graphene functionalization,

Res. Chem. Intermed. 44 (2018) 3523–3536. https://doi.org/10.1007/s11164-018-3322-3.

[119] Y. Dong, J. Li, L. Shi, J. Xu, X. Wang, Z. Guo, W. Liu, Graphene oxide-iron complex: Synthesis, characterization and visible-light-driven photocatalysis, J. Mater. Chem. A. 1 (2013) 644–650. https://doi.org/10.1039/c2ta00371f.

[120] A.F. De Faria, D.S.T. Martinez, S.M.M. Meira, A.C.M. de Moraes, A. Brandelli, A.G.S. Filho, O.L. Alves, Anti-adhesion and antibacterial activity of silver nanoparticles supported on graphene oxide sheets, Colloids Surfaces B Biointerfaces. 113 (2014) 115–124. https://doi.org/10.1016/j.colsurfb.2013.08.006.

[121] T.T. Baby, S. Ramaprabhu, Synthesis and nanofluid application of silver nanoparticles decorated graphene, J. Mater. Chem. 21 (2011) 9702–9709. https://doi.org/10.1039/c0jm04106h.

[122] S.C. Lin, C.C.M. Ma, S.T. Hsiao, Y.S. Wang, C.Y. Yang, W.H. Liao, S.M. Li, J.A. Wang, T.Y. Cheng, C.W. Lin, R. Bin Yang, Electromagnetic interference shielding performance of waterborne polyurethane composites filled with silver nanoparticles deposited on functionalized graphene, Appl. Surf. Sci. 385 (2016) 436–444. https://doi.org/10.1016/j.apsusc.2016.05.063.

[123] S.V. Kumar, N.M. Huang, H.N. Lim, M. Zainy, I. Harrison, C.H. Chia, Preparation of highly water dispersible functional graphene/silver nanocomposite for the detection of melamine, Sensors Actuators, B Chem. 181 (2013) 885–893. https://doi.org/10.1016/j.snb.2013.02.045.

[124] A. Moradi Golsheikh, N.M. Huang, H.N. Lim, R. Zakaria, C.Y. Yin, One-step electrodeposition synthesis of silver-nanoparticle-decorated graphene on indium-tin-oxide for enzymeless hydrogen peroxide detection, Carbon N. Y. 62 (2013) 405–412.

https://doi.org/10.1016/j.carbon.2013.06.025.

[125] P. Chettri, V.S. Vendamani, A. Tripathi, M.K. Singh, A.P. Pathak, A. Tiwari, Green synthesis of silver nanoparticle-reduced graphene oxide using Psidium guajava and its application in SERS for the detection of methylene blue, Appl. Surf. Sci. 406 (2017) 312–318. https://doi.org/10.1016/j.apsusc.2017.02.073.

[126] K.J. Huang, Y.J. Liu, H.B. Wang, Y.Y. Wang, A sensitive electrochemical DNA biosensor based on silver nanoparticles-polydopamine@graphene composite, Electrochim. Acta. 118 (2014) 130–137. https://doi.org/10.1016/j.electacta.2013.12.019.

[127] E.S. Orth, J.E.S. Fonsaca, S.H. Domingues, H. Mehl, M.M. Oliveira, A.J.G. Zarbin, Targeted thiolation of graphene oxide and its utilization as precursor for graphene/silver nanoparticles composites, Carbon N. Y. 61 (2013) 543–550. https://doi.org/10.1016/j.carbon.2013.05.032.

[128] A.O.E. Abdelhalim, A. Galal, M.Z. Hussein, I.E.T. El Sayed, Graphene Functionalization by 1,6-Diaminohexane and Silver Nanoparticles for Water Disinfection, J. Nanomater. 2016 (2016). https://doi.org/10.1155/2016/1485280.

[129] G. Goncalves, P.A.A.P. Marques, C.M. Granadeiro, H.I.S. Nogueira, M.K. Singh, J. Grácio, Surface modification of graphene nanosheets with gold nanoparticles: The role of oxygen moieties at graphene surface on gold nucleation and growth, Chem. Mater. 21 (2009) 4796–4802. https://doi.org/10.1021/cm901052s.

[130] T.A. Pham, B.C. Choi, K.T. Lim, Y.T. Jeong, A simple approach for immobilization of gold nanoparticles on graphene oxide sheets by covalent bonding, Appl. Surf. Sci. 257 (2011) 3350–3357. https://doi.org/10.1016/j.apsusc.2010.11.023.

[131] K. Chen, G. Lu, J. Chang, S. Mao, K. Yu, S. Cui, J. Chen, Hg(II) ion detection using

thermally reduced graphene oxide decorated with functionalized gold nanoparticles, Anal. Chem. 84 (2012) 4057–4062. https://doi.org/10.1021/ac3000336.

[132] Y.K. Kim, H.K. Na, D.H. Min, Influence of surface functionalization on the growth of gold nanostructures on graphene thin films, Langmuir. 26 (2010) 13065–13070. https://doi.org/10.1021/la102372z.

[133] H. Zhang, D. Hines, D.L. Akins, Synthesis of a nanocomposite composed of reduced graphene oxide and gold nanoparticles, Dalt. Trans. 43 (2014) 2670–2675. https://doi.org/10.1039/c3dt52573b.

[134] J. Liu, Adsorption of DNA onto gold nanoparticles and graphene oxide: Surface science and applications, Phys. Chem. Chem. Phys. 14 (2012) 10485–10496. https://doi.org/10.1039/c2cp41186e.

[135] R.K. Biroju, P.K. Giri, Defect enhanced efficient physical functionalization of graphene with gold nanoparticles probed by resonance Raman spectroscopy, J. Phys. Chem. C. 118 (2014) 13833–13843. https://doi.org/10.1021/jp500501e.

[136] I. Khalil, N. Julkapli, W. Yehye, W. Basirun, S. Bhargava, Graphene–Gold Nanoparticles Hybrid—Synthesis, Functionalization, and Application in a Electrochemical and Surface-Enhanced Raman Scattering Biosensor, Materials (Basel). 9 (2016) 406. https://doi.org/10.3390/ma9060406.

[137] D. He, K. Cheng, H. Li, T. Peng, F. Xu, S. Mu, M. Pan, Highly active platinum nanoparticles on graphene nanosheets with a significant improvement in stability and CO tolerance, Langmuir. 28 (2012) 3979–3986. https://doi.org/10.1021/la2045493.

[138] D. Marquardt, F. Beckert, F. Pennetreau, F. Tölle, R. Mülhaupt, O. Riant, S. Hermans, J. Barthel, C. Janiak, Hybrid materials of platinum nanoparticles and thiol-functionalized

graphene derivatives, Carbon N. Y. 66 (2014) 285–294. https://doi.org/10.1016/j.carbon.2013.09.002.

[139] L. Xin, F. Yang, S. Rasouli, Y. Qiu, Z.F. Li, A. Uzunoglu, C.J. Sun, Y. Liu, P. Ferreira, W. Li, Y. Ren, L.A. Stanciu, J. Xie, Understanding Pt Nanoparticle Anchoring on Graphene Supports through Surface Functionalization, ACS Catal. 6 (2016) 2642–2653. https://doi.org/10.1021/acscatal.5b02722.

[140] L.I. Şanli, V. Bayram, B. Yarar, S. Ghobadi, S.A. Gürsel, Development of graphene supported platinum nanoparticles for polymer electrolyte membrane fuel cells: Effect of support type and impregnation-reduction methods, Int. J. Hydrogen Energy. 41 (2016) 3414–3427. https://doi.org/10.1016/j.ijhydene.2015.12.166.

[141] R.X. Wang, J.J. Fan, Y.J. Fan, J.P. Zhong, L. Wang, S.G. Sun, X.C. Shen, Platinum nanoparticles on porphyrin functionalized graphene nanosheets as a superior catalyst for methanol electrooxidation, Nanoscale. 6 (2014) 14999–15007. https://doi.org/10.1039/c4nr04140b.

[142] J. Lu, Y. Li, S. Li, S.P. Jiang, Self-assembled platinum nanoparticles on sulfonic acid-grafted graphene as effective electrocatalysts for methanol oxidation in direct methanol fuel cells, Sci. Rep. 6 (2016) 1–12. https://doi.org/10.1038/srep21530.

[143] S.S. Low, H.S. Loh, J.S. Boey, P.S. Khiew, W.S. Chiu, M.T.T. Tan, Sensitivity enhancement of graphene/zinc oxide nanocomposite-based electrochemical impedance genosensor for single stranded RNA detection, Biosens. Bioelectron. 94 (2017) 365–373. https://doi.org/10.1016/j.bios.2017.02.038.

[144] V. Galstyan, E. Comini, I. Kholmanov, G. Faglia, G. Sberveglieri, Reduced graphene oxide/ZnO nanocomposite for application in chemical gas sensors, RSC Adv. 6 (2016)

34225–34232. https://doi.org/10.1039/c6ra01913g.

[145] M.K. Kavitha, H. John, P. Gopinath, R. Philip, Synthesis of reduced graphene oxide-ZnO hybrid with enhanced optical limiting properties, J. Mater. Chem. C. 1 (2013) 3669–3676. https://doi.org/10.1039/c3tc30323c.

[146] R.S. Rajaura, V. Sharma, R.S. Ronin, D.K. Gupta, S. Srivastava, K. Agrawal, Y.K. Vijay, Synthesis, characterization and enhanced antimicrobial activity of reduced graphene oxide-zinc oxide nanocomposite, Mater. Res. Express. 4 (2017) 025401. https://doi.org/10.1088/2053-1591/aa5bff.

[147] N. Yusoff, N.M. Huang, M.R. Muhamad, S. V. Kumar, H.N. Lim, I. Harrison, Hydrothermal synthesis of CuO/functionalized graphene nanocomposites for dye degradation, Mater. Lett. 93 (2013) 393–396. https://doi.org/10.1016/j.matlet.2012.10.015.

[148] P. Rajapaksha, S. Cheeseman, S. Hombsch, B.J. Murdoch, S. Gangadoo, E.W. Blanch, Y. Truong, D. Cozzolino, C.F. McConville, R.J. Crawford, V.K. Truong, A. Elbourne, J. Chapman, Antibacterial Properties of Graphene Oxide-Copper Oxide Nanoparticle Nanocomposites, ACS Appl. Bio Mater. 2 (2019) 5687–5696. https://doi.org/10.1021/acsabm.9b00754.

[149] N.V.S. Vallabani, S. Singh, Recent advances and future prospects of iron oxide nanoparticles in biomedicine and diagnostics, 3 Biotech. 8 (2018) 279. https://doi.org/10.1007/s13205-018-1286-z.

[150] S. Bandi, V. Hastak, C.L.P. Pavithra, S. Kashyap, D.K. Singh, S. Luqman, D.R. Peshwe, A.K. Srivastav, Graphene/chitosan-functionalized iron oxide nanoparticles for biomedical applications, J. Mater. Res. 34 (2019) 3389–3399. https://doi.org/10.1557/jmr.2019.267.

[151] Y. Zhang, B. Chen, L. Zhang, J. Huang, F. Chen, Z. Yang, J. Yao, Z. Zhang, Controlled assembly of Fe3O4 magnetic nanoparticles on graphene oxide, Nanoscale. 3 (2011) 1446–1450. https://doi.org/10.1039/c0nr00776e.

[152] A.K. Gupta, R.R. Naregalkar, V.D. Vaidya, M. Gupta, Recent advances on surface engineering of magnetic iron oxide nanoparticles and their biomedical applications, Nanomedicine. 2 (2007) 23–39. https://doi.org/10.2217/17435889.2.1.23.

[153] F. He, J. Fan, D. Ma, L. Zhang, C. Leung, H.L. Chan, The attachment of Fe3O4 nanoparticles to graphene oxide by covalent bonding, Carbon N. Y. 48 (2010) 3139–3144. https://doi.org/10.1016/j.carbon.2010.04.052.

[154] R. Gonzalez-Rodriguez, E. Campbell, A. Naumov, Multifunctional graphene oxide/iron oxide nanoparticles for magnetic targeted drug delivery dual magnetic resonance/ fluorescence imaging and cancer sensing, PLoS One. 14 (2019) e0217072. https://doi.org/10.1371/journal.pone.0217072.

[155] M. Fang, K. Wang, H. Lu, Y. Yang, S. Nutt, Covalent polymer functionalization of graphene nanosheets and mechanical properties of composites, J. Mater. Chem. 19 (2009) 7098–7105. https://doi.org/10.1039/b908220d.

[156] H. Nguyen Bich, H. Nguyen Van, Promising applications of graphene and graphene-based nanostructures, Adv. Nat. Sci. Nanosci. Nanotechnol. 7 (2016) 15. https://doi.org/10.1088/2043-6262/7/2/023002.

[157] K. Tadyszak, J. Wychowaniec, J. Litowczenko, Biomedical Applications of Graphene-Based Structures, Nanomaterials. 8 (2018) 944. https://doi.org/10.3390/nano8110944.

[158] C. Chung, Y.K. Kim, D. Shin, S.R. Ryoo, B.H. Hong, D.H. Min, Biomedical applications of graphene and graphene oxide, Acc. Chem. Res. 46 (2013) 2211–2224.

https://doi.org/10.1021/ar300159f.

[159] M. Fang, K. Wang, H. Lu, Y. Yang, S. Nutt, Covalent polymer functionalization of graphene nanosheets and mechanical properties of composites, J. Mater. Chem. 19 (2009) 7098–7105. https://doi.org/10.1039/b908220d.

[160] M. Cano, U. Khan, T. Sainsbury, A. O'Neill, Z. Wang, I.T. McGovern, W.K. Maser, A.M. Benito, J.N. Coleman, Improving the mechanical properties of graphene oxide based materials by covalent attachment of polymer chains, Carbon N. Y. 52 (2013) 363–371. https://doi.org/10.1016/j.carbon.2012.09.046.

[161] Y.J. Wan, L.C. Tang, L.X. Gong, D. Yan, Y.B. Li, L. Bin Wu, J.X. Jiang, G.Q. Lai, Grafting of epoxy chains onto graphene oxide for epoxy composites with improved mechanical and thermal properties, Carbon N. Y. 69 (2014) 467–480. https://doi.org/10.1016/j.carbon.2013.12.050.

[162] X. Zhiyuan, X. Zhiyuan, W. Song, L. Yongjun, W. Mingwei, S. Ping, H. Xiaoyu, Covalent Functionalization of Graphene Oxide with Biocompatible Poly(ethylene glycol) for Delivery of Paclitaxel, ACS Appl. Mater. Interfaces. 6 (2014) 17268–17276. https://jglobal.jst.go.jp/en/detail?JGLOBAL_ID=201402233216087107 (accessed June 29, 2020).

[163] B.C. Mei, K. Susumu, I.L. Medintz, J.B. Delehanty, T.J. Mountziaris, H. Mattoussi, Modular poly(ethylene glycol) ligands for biocompatible semiconductor and gold nanocrystals with extended pH and ionic stability, J. Mater. Chem. 18 (2008) 4949–4958. https://doi.org/10.1039/b810488c.

[164] Y.H. Yu, Y.Y. Lin, C.H. Lin, C.C. Chan, Y.C. Huang, High-performance polystyrene/graphene-based nanocomposites with excellent anti-corrosion properties,

Polym. Chem. 5 (2014) 535–550. https://doi.org/10.1039/c3py00825h.

[165] K. Deshmukh, S.M. Khatake, G.M. Joshi, Surface properties of graphene oxide reinforced polyvinyl chloride nanocomposites, J. Polym. Res. 20 (2013) 1–11. https://doi.org/10.1007/s10965-013-0286-2.

[166] E.A. Ovcharenko, A. Seifalian, M.A. Rezvova, K.Y. Klyshnikov, T.V. V. Glushkova, T.N. Akenteva, L.V. V. Antonova, E.A. Velikanova, V.S. Chernonosova, G.Y. Shevelev, D.K. Shishkova, E.O. Krivkina, Y.A. Kudryavceva, A.M. Seifalian, L.S. Barbarash, A New Nanocomposite Copolymer Based On Functionalised Graphene Oxide for Development of Heart Valves, Sci. Rep. 10 (2020). https://doi.org/10.1038/s41598-020-62122-8.

[167] R. Kumar, M. Mamlouk, K. Scott, Sulfonated polyether ether ketone-sulfonated graphene oxide composite membranes for polymer electrolyte fuel cells, RSC Adv. 4 (2014) 617–623. https://doi.org/10.1039/c3ra42390e.

[168] L. Zhang, J. Xia, Q. Zhao, L. Liu, Z. Zhang, Functional Graphene Oxide as a Nanocarrier for Controlled Loading and Targeted Delivery of Mixed Anticancer Drugs, Small. 6 (2010) 537–544. https://doi.org/10.1002/smll.200901680.

[169] L. Fan, H. Ge, S. Zou, Y. Xiao, H. Wen, Y. Li, H. Feng, M. Nie, Sodium alginate conjugated graphene oxide as a new carrier for drug delivery system, Int. J. Biol. Macromol. 93 (2016) 582–590. https://doi.org/10.1016/j.ijbiomac.2016.09.026.

[170] X.C. Qin, Z.Y. Guo, Z.M. Liu, W. Zhang, M.M. Wan, B.W. Yang, Folic acid-conjugated graphene oxide for cancer targeted chemo-photothermal therapy, J. Photochem. Photobiol. B Biol. 120 (2013) 156–162. https://doi.org/10.1016/j.jphotobiol.2012.12.005.

[171] P. Huang, C. Xu, J. Lin, C. Wang, X. Wang, C. Zhang, X. Zhou, S. Guo, D. Cui, Folic

Acid-conjugated Graphene Oxide loaded with Photosensitizers for Targeting Photodynamic Therapy, Theranostics. 1 (2012) 240–250. https://doi.org/10.7150/thno/v01p0240.

[172] H. Tiwari, N. Karki, M. Pal, S. Basak, R.K. Verma, R. Bal, N.D. Kandpal, G. Bisht, N.G. Sahoo, Functionalized graphene oxide as a nanocarrier for dual drug delivery applications: The synergistic effect of quercetin and gefitinib against ovarian cancer cells, Colloids Surfaces B Biointerfaces. 178 (2019) 452–459. https://doi.org/10.1016/j.colsurfb.2019.03.037.

[173] A. Deb, R. Vimala, Camptothecin loaded graphene oxide nanoparticle functionalized with polyethylene glycol and folic acid for anticancer drug delivery, J. Drug Deliv. Sci. Technol. 43 (2018) 333–342. https://doi.org/10.1016/j.jddst.2017.10.025.

[174] M. Pooresmaeil, H. Namazi, β-Cyclodextrin grafted magnetic graphene oxide applicable as cancer drug delivery agent: Synthesis and characterization, Mater. Chem. Phys. 218 (2018) 62–69. https://doi.org/10.1016/j.matchemphys.2018.07.022.

[175] A. Deb, N.G. Andrews, V. Raghavan, Natural polymer functionalized graphene oxide for co-delivery of anticancer drugs: In-vitro and in-vivo, Int. J. Biol. Macromol. 113 (2018) 515–525. https://doi.org/10.1016/j.ijbiomac.2018.02.153.

[176] X. Pei, Z. Zhu, Z. Gan, J. Chen, X. Zhang, X. Cheng, Q. Wan, J. Wang, PEGylated nano-graphene oxide as a nanocarrier for delivering mixed anticancer drugs to improve anticancer activity, Sci. Rep. 10 (2020) 1–15. https://doi.org/10.1038/s41598-020-59624-w.

[177] S. Bullo, K. Buskaran, R. Baby, D. Dorniani, S. Fakurazi, M.Z. Hussein, Dual Drugs Anticancer Nanoformulation using Graphene Oxide-PEG as Nanocarrier for

Protocatechuic Acid and Chlorogenic Acid, Pharm. Res. 36 (2019) 91. https://doi.org/10.1007/s11095-019-2621-8.

[178] P. Gong, Q. Zhao, D. Dai, S. Zhang, Z. Tian, L. Sun, J. Ren, Z. Liu, Functionalized Ultrasmall Fluorinated Graphene with High NIR Absorbance for Controlled Delivery of Mixed Anticancer Drugs, Chem. - A Eur. J. 23 (2017) 17531–17541. https://doi.org/10.1002/chem.201702917.

[179] P. Gong, J. Du, D. Wang, B. Cao, M. Tian, Y. Wang, L. Sun, S. Ji, Z. Liu, Fluorinated graphene as an anticancer nanocarrier: An experimental and DFT study, J. Mater. Chem. B. 6 (2018) 2769–2777. https://doi.org/10.1039/c8tb00102b.

[180] G. Shim, J.Y. Kim, J. Han, S.W. Chung, S. Lee, Y. Byun, Y.K. Oh, Reduced graphene oxide nanosheets coated with an anti-angiogenic anticancer low-molecular-weight heparin derivative for delivery of anticancer drugs, J. Control. Release. 189 (2014) 80–89. https://doi.org/10.1016/j.jconrel.2014.06.026.

[181] Y. Zhang, C. Wu, J. Zhang, Interactions of graphene and graphene oxide with proteins and peptides, Nanotechnol. Rev. 2 (2013) 27–45. https://doi.org/10.1515/ntrev-2012-0078.

[182] Y. Zhang, J. Zhang, X. Huang, X. Zhou, H. Wu, S. Guo, Assembly of graphene oxide-enzyme conjugates through hydrophobic interaction, Small. 8 (2012) 154–159. https://doi.org/10.1002/smll.201101695.

[183] J. Wang, M. Cheng, Z. Zhang, L. Guo, Q. Liu, G. Jiang, An antibody-graphene oxide nanoribbon conjugate as a surface enhanced laser desorption/ionization probe with high sensitivity and selectivity, Chem. Commun. 51 (2015) 4619–4622. https://doi.org/10.1039/c4cc10401c.

[184] S. Jokar, A. Pourjavadi, M. Adeli, Albumin-graphene oxide conjugates; Carriers for

anticancer drugs, RSC Adv. 4 (2014) 33001–33006. https://doi.org/10.1039/c4ra05752j.

[185] H. Kim, R. Namgung, K. Singha, I.K. Oh, W.J. Kim, Graphene oxide-polyethylenimine nanoconstruct as a gene delivery vector and bioimaging tool, Bioconjug. Chem. 22 (2011) 2558–2567. https://doi.org/10.1021/bc200397j.

[186] A.O.E. Abdelhalim, V. V. Sharoyko, A.A. Meshcheriakov, M.D. Luttsev, A.A. Potanin, N.R. Iamalova, E.E. Zakharov, S. V. Ageev, A. V. Petrov, L. V. Vasina, I.L. Solovtsova, A. V. Nashchekin, I. V. Murin, K.N. Semenov, Synthesis, characterisation and biocompatibility of graphene–L-methionine nanomaterial, J. Mol. Liq. 314 (2020) 113605. https://doi.org/10.1016/j.molliq.2020.113605.

[187] A.O.E. Abdelhalim, V. V. Sharoyko, A.A. Meshcheriakov, S.D. Martynova, S. V. Ageev, G.O. Iurev, H. Al Mulla, A. V. Petrov, I.L. Solovtsova, L. V. Vasina, I. V. Murin, K.N. Semenov, Reduction and functionalization of graphene oxide with L-cysteine: Synthesis, characterization and biocompatibility, Nanomedicine Nanotechnology, Biol. Med. 29 (2020) 102284. https://doi.org/10.1016/j.nano.2020.102284.

[188] D. Manoj, K. Theyagarajan, D. Saravanakumar, S. Senthilkumar, K. Thenmozhi, Aldehyde functionalized ionic liquid on electrochemically reduced graphene oxide as a versatile platform for covalent immobilization of biomolecules and biosensing, Biosens. Bioelectron. 103 (2018) 104–112. https://doi.org/10.1016/j.bios.2017.12.030.

[189] S.M. Mousavi, S.A. Hashemi, Y. Ghasemi, A.M. Amani, A. Babapoor, O. Arjmand, Applications of graphene oxide in case of nanomedicines and nanocarriers for biomolecules: review study, Drug Metab. Rev. 51 (2019) 12–41. https://doi.org/10.1080/03602532.2018.1522328.

[190] D. Li, W. Zhang, X. Yu, Z. Wang, Z. Su, G. Wei, When biomolecules meet graphene:

From molecular level interactions to material design and applications, Nanoscale. 8 (2016) 19491–19509. https://doi.org/10.1039/c6nr07249f.

[191] W. Deng, X. Yuan, Y. Tan, M. Ma, Q. Xie, Three-dimensional graphene-like carbon frameworks as a new electrode material for electrochemical determination of small biomolecules, Biosens. Bioelectron. 85 (2016) 618–624. https://doi.org/10.1016/j.bios.2016.05.065.

[192] H. Wang, K. Ma, B. Xu, W. Tian, Tunable Supramolecular Interactions of Aggregation-Induced Emission Probe and Graphene Oxide with Biomolecules: An Approach toward Ultrasensitive Label-Free and "Turn-On" DNA Sensing, Small. 12 (2016) 6613–6622. https://doi.org/10.1002/smll.201601544.

[193] C.F. Wang, X.Y. Sun, M. Su, Y.P. Wang, Y.K. Lv, Electrochemical biosensors based on antibody, nucleic acid and enzyme functionalized graphene for the detection of disease-related biomolecules, Analyst. 145 (2020) 1550–1562. https://doi.org/10.1039/c9an02047k.

[194] L. Lu, Recent advances in synthesis of three-dimensional porous graphene and its applications in construction of electrochemical (bio)sensors for small biomolecules detection, Biosens. Bioelectron. 110 (2018) 180–192. https://doi.org/10.1016/j.bios.2018.03.060.

[195] Z. Nan, C. Hao, X. Ye, Y. Feng, R. Sun, Interaction of graphene oxide with bovine serum albumin: A fluorescence quenching study, Spectrochim. Acta - Part A Mol. Biomol. Spectrosc. 210 (2019) 348–354. https://doi.org/10.1016/j.saa.2018.11.028.

[196] H. Zhang, Z. Zhu, Y. Wang, Z. Fei, J. Cao, Changing the activities and structures of bovine serum albumin bound to graphene oxide, Appl. Surf. Sci. 427 (2018) 1019–1029.

https://doi.org/10.1016/j.apsusc.2017.08.130.

[197] C. Lu, P.J. Jimmy Huang, Y. Ying, J. Liu, Covalent linking DNA to graphene oxide and its comparison with physisorbed probes for Hg2+ detection, Biosens. Bioelectron. 79 (2016) 244–250. https://doi.org/10.1016/j.bios.2015.12.043.

[198] K.H. Liao, Y.S. Lin, C.W. MacOsko, C.L. Haynes, Cytotoxicity of graphene oxide and graphene in human erythrocytes and skin fibroblasts, ACS Appl. Mater. Interfaces. 3 (2011) 2607–2615. https://doi.org/10.1021/am200428v.

[199] P. AM, M. JA, M. FD, G. IC, Polymer surface adsorption as a strategy to improve the biocompatibility of graphene nanoplatelets, Colloids Surf. B. Biointerfaces. 146 (2016) 818–824. https://doi.org/10.1016/J.COLSURFB.2016.07.031.

[200] A. AOE, S. VV, A. SV, F. VS, N. DA, P. VN, P. AV, S. KN, Graphene Oxide of Extra High Oxidation: A Wafer for Loading Guest Molecules, J. Phys. Chem. Lett. (2021) 10015–10024. https://doi.org/10.1021/ACS.JPCLETT.1C02766.

[201] S.K. Singh, M.K. Singh, P.P. Kulkarni, V.K. Sonkar, J.J.A. Grácio, D. Dash, Amine-modified graphene: Thrombo-protective safer alternative to graphene oxide for biomedical applications, ACS Nano. 6 (2012) 2731–2740. https://doi.org/10.1021/nn300172t.

[202] S.K. Singh, M.K. Singh, M.K. Nayak, S. Kumari, S. Shrivastava, J.J.A. Grácio, D. Dash, Thrombus inducing property of atomically thin graphene oxide sheets, ACS Nano. 5 (2011) 4987–4996. https://doi.org/10.1021/nn201092p.

[203] M.J. Podolska, A. Barras, C. Alexiou, B. Frey, U. Gaipl, R. Boukherroub, S. Szunerits, C. Janko, L.E. Muñoz, Graphene Oxide Nanosheets for Localized Hyperthermia—Physicochemical Characterization, Biocompatibility, and Induction of Tumor Cell Death, Cells 2020, Vol. 9, Page 776. 9 (2020) 776. https://doi.org/10.3390/CELLS9030776.

[204] Z. Ding, H. Ma, Y. Chen, Interaction of graphene oxide with human serum albumin and its mechanism, RSC Adv. 4 (2014) 55290–55295. https://doi.org/10.1039/c4ra09613d.

[205] S.G. Taneva, S. Krumova, F. Bogár, A. Kincses, S. Stoichev, S. Todinova, A. Danailova, J. Horváth, Z. Násztor, L. Kelemen, A. Dér, Insights into graphene oxide interaction with human serum albumin in isolated state and in blood plasma, Int. J. Biol. Macromol. 175 (2021) 19–29. https://doi.org/10.1016/J.IJBIOMAC.2021.01.151.

[206] L. Y, L. Y, W. J, W. Y, Y. X, Y. R, W. B, Y. J, Z. N, Graphene oxide can induce in vitro and in vivo mutagenesis, Sci. Rep. 3 (2013). https://doi.org/10.1038/SREP03469.

[207] A. Wang, K. Pu, B. Dong, Y. Liu, L. Zhang, Z. Zhang, W. Duan, Y. Zhu, Role of surface charge and oxidative stress in cytotoxicity and genotoxicity of graphene oxide towards human lung fibroblast cells, (2013). https://doi.org/10.1002/jat.2877.

[208] O. Akhavan, E. Ghaderi, A. Akhavan, Size-dependent genotoxicity of graphene nanoplatelets in human stem cells, Biomaterials. 33 (2012) 8017–8025. https://doi.org/10.1016/j.biomaterials.2012.07.040.

[209] Abdelsattar O. E. Abdelhalim, K.N. Semenov, D.A. Nerukh, I. V. Murin, O.E.M. Dmitrii N. Maistrenko, V. V. Sharoyko, Graphene oxide enriched with oxygen-containing groups: on the way to an increase of antioxidant activity and biocompatibility, Colloids Surfaces B Biointerfaces. (2021).

[210] Y. Wang, S. Wu, X. Zhao, Z. Su, L. Du, A. Sui, In vitro toxicity evaluation of graphene oxide on human RPMI 8226 cells, in: Biomed. Mater. Eng., IOS Press, 2014: pp. 2007–2013. https://doi.org/10.3233/BME-141010.

[211] J. Sun, Y. Deng, J. Li, G. Wang, P. He, S. Tian, X. Bu, Z. Di, S. Yang, G. Ding, X. Xie, A New Graphene Derivative: Hydroxylated Graphene with Excellent Biocompatibility,

(2016). https://doi.org/10.1021/acsami.6b02032.

[212] H. Wu, H. Shi, Y. Wang, X. Jia, C. Tang, J. Zhang, S. Yang, Hyaluronic acid conjugated graphene oxide for targeted drug delivery, Carbon N. Y. (2013). https://doi.org/10.1016/j.carbon.2013.12.039.

[213] Y. Si, E.T. Samulski, Synthesis of Water Soluble Graphene, (n.d.). https://doi.org/10.1021/nl080604h.

[214] V. V. Neklyudov, N.R. Khafizov, I.A. Sedov, A.M. Dimiev, New insights into the solubility of graphene oxide in water and alcohols, Phys. Chem. Chem. Phys. 19 (2017) 17000–17008. https://doi.org/10.1039/C7CP02303K.

[215] M. Lotya, Y. Hernandez, P.J. King, R.J. Smith, V. Nicolosi, L.S. Karlsson, F.M. Blighe, S. De, Z. Wang, I.T. McGovern, G.S. Duesberg, J.N. Coleman, Liquid Phase Production of Graphene by Exfoliation of Graphite in Surfactant/Water Solutions, J. Am. Chem. Soc. 131 (2009) 3611–3620. https://doi.org/10.1021/JA807449U.

[216] S. Lin, C.-J. Shih, M.S. Strano, D. Blankschtein, Molecular Insights into the Surface Morphology, Layering Structure, and Aggregation Kinetics of Surfactant-Stabilized Graphene Dispersions, J. Am. Chem. Soc. 133 (2011) 12810–12823. https://doi.org/10.1021/JA2048013.

[217] X. Li, Y. Chen, S. Mo, L. Jia, X. Shao, Effect of surface modification on the stability and thermal conductivity of water-based SiO 2-coated graphene nanofluid, (2014). https://doi.org/10.1016/j.tca.2014.09.006.

[218] O. V. Kharissova, C.M. Oliva González, B.I. Kharisov, Solubilization and Dispersion of Carbon Allotropes in Water and Non-aqueous Solvents, Ind. Eng. Chem. Res. 57 (2018) 12624–12645. https://doi.org/10.1021/ACS.IECR.8B02593.

[219] C. Lee, X. Wei, J. Kysar, J.H.- science, undefined 2008, Measurement of the elastic properties and intrinsic strength of monolayer graphene, Science.Sciencemag.Org. 54 (2006) 635. https://doi.org/10.1126/science.1156211.

[220] A. Teklu, C. Barry, M. Palumbo, C. Weiwadel, N. Kuthirummal, J. Flagg, H. Fang, Mechanical Characterization of Reduced Graphene Oxide Using AFM, Adv. Condens. Matter Phys. 2019 (2019). https://doi.org/10.1155/2019/8713965.

[221] C. Gómez-Navarro, M. Burghard, K. Kern, Elastic Properties of Chemically Derived Single Graphene Sheets, NANO Lett. 8 (2008) 2045–2049. https://doi.org/10.1021/nl801384y.

[222] H. Chen, M.B. Müller, K.J. Gilmore, G.G. Wallace, D. Li, Mechanically Strong, Electrically Conductive, and Biocompatible Graphene Paper, Adv. Mater. 20 (2008) 3557–3561. https://doi.org/10.1002/ADMA.200800757.

[223] J.W. Suk, R.D. Piner, J. An, R.S. Ruoff, Mechanical Properties of Monolayer Graphene Oxide, ACS Nano. 4 (2010) 6557–6564. https://doi.org/10.1021/NN101781V.

[224] C. Cao, M. Daly, C.V. Singh, Y. Sun, T. Filleter, High strength measurement of monolayer graphene oxide, Carbon N. Y. C (2015) 497–504. https://doi.org/10.1016/J.CARBON.2014.09.082.

[225] P. S, R. RS, Chemical methods for the production of graphenes, Nat. Nanotechnol. 4 (2009) 217–224. https://doi.org/10.1038/NNANO.2009.58.

[226] N. KS, F. VI, C. L, G. PR, S. MG, K. K, A roadmap for graphene., Nature. 490 (2012) 192–200. https://doi.org/10.1038/NATURE11458.

[227] S. Thakur, N. Karak, Green reduction of graphene oxide by aqueous phytoextracts, Carbon N. Y. 50 (2012) 5331–5339. https://doi.org/10.1016/j.carbon.2012.07.023.

[228] S. Gupta, P. Joshi, J. Narayan, Electron mobility modulation in graphene oxide by controlling carbon melt lifetime, Carbon N. Y. 170 (2020) 327–337. https://doi.org/10.1016/J.CARBON.2020.07.073.

[229] S. Pei, J. Zhao, J. Du, W. Ren, H.-M. Cheng, Direct reduction of graphene oxide films into highly conductive and flexible graphene films by hydrohalic acids, Carbon N. Y. 48 (2010) 4466–4474. https://doi.org/10.1016/j.carbon.2010.08.006.

[230] Y. Sim, S. Surendran, H. Cha, H. Choi, M. Je, S. Yoo, D. Chan Seok, Y. Ho Jung, C. Jeon, D. Jin Kim, M.K. Han, H. Choi, U. Sim, J. Moon, Fluorine-doped graphene oxide prepared by direct plasma treatment for supercapacitor application, Chem. Eng. J. 428 (2022) 132086. https://doi.org/10.1016/J.CEJ.2021.132086.

[231] G. Eda, G. Fanchini, M. Chhowalla, Large-area ultrathin films of reduced graphene oxide as a transparent and flexible electronic material, Nat. Nanotechnol. 2008 35. 3 (2008) 270–274. https://doi.org/10.1038/nnano.2008.83.

[232] S.H. Kang, T.H. Fang, Z.H. Hong, Electrical and mechanical properties of graphene oxide on flexible substrate, J. Phys. Chem. Solids. 74 (2013) 1783–1793. https://doi.org/10.1016/J.JPCS.2013.07.009.

[233] L.A. Jauregui, Y. Yue, A.N. Sidorov, J. Hu, Q. Yu, G. Lopez, R. Jalilian, D.K. Benjamin, D.A. Delk, W. Wu, Z. Liu, X. Wang, Z. Jiang, X. Ruan, J. Bao, S.S. Pei, Y.P. Chen, Thermal Transport in Graphene Nanostructures: Experiments and Simulations, (n.d.). https://doi.org/10.1149/1.3367938.

[234] S. Joshi, J. Lee, G.K.-M. Letters, undefined 2021, Low-cost synthesis of high quality graphene oxide with large electrical and thermal conductivities, Elsevier. (n.d.). https://www.sciencedirect.com/science/article/pii/S0167577X21003451 (accessed October

25, 2021).

[235] X. Mu, X. Wu, T. Zhang, D.B. Go, T. Luo, Thermal Transport in Graphene Oxide-From Ballistic Extreme to Amorphous Limit, (2014). https://doi.org/10.1038/srep03909.

[236] H. Shen, L. Zhang, M. Liu, Z. Zhang, Biomedical Applications of Graphene, Theranostics. 2 (2012) 283. https://doi.org/10.7150/THNO.3642.

[237] P. Avouris, F. Xia, Graphene applications in electronics and photonics, MRS Bull. 37 (2012) 1225–1234. https://doi.org/10.1557/mrs.2012.206.

[238] A.T. Lawal, Graphene-based nano composites and their applications. A review, Biosens. Bioelectron. 141 (2019) 111384. https://doi.org/10.1016/J.BIOS.2019.111384.

[239] P.K. Sandhya, J. Jose, M.S. Sreekala, M. Padmanabhan, N. Kalarikkal, S. Thomas, Reduced graphene oxide and ZnO decorated graphene for biomedical applications, Ceram. Int. 44 (2018) 15092–15098. https://doi.org/10.1016/J.CERAMINT.2018.05.143.

[240] J. Zhao, R. Pan, R. Sun, C. Wen, S.L. Zhang, B. Wu, L. Nyholm, Z. Bin Zhang, High-conductivity reduced-graphene-oxide/copper aerogel for energy storage, Nano Energy. 60 (2019) 760–767. https://doi.org/10.1016/J.NANOEN.2019.04.023.

[241] M. Soni, P. Kumar, J. Pandey, S.K. Sharma, A. Soni, Scalable and site specific functionalization of reduced graphene oxide for circuit elements and flexible electronics, Carbon N. Y. 128 (2018) 172–178. https://doi.org/10.1016/J.CARBON.2017.11.087.

[242] Z. Wang, X. Zhan, Y. Wang, S. Muhammad, Y. Huang, J. He, A flexible UV nanosensor based on reduced graphene oxide decorated ZnO nanostructures, Nanoscale. 4 (2012) 2678–2684. https://doi.org/10.1039/C2NR30354J.

[243] D.C. Sekhar, B.S. Diwakar, B.R. Babu, N. Madhavi, Development of graphene oxide based hybrid metal oxide nanocomposites of GO-SnO2/ZnO/Fe3O4, GO-

SiO2/ZnO/Fe3O4 for energy applications, Phys. B Condens. Matter. 603 (2021) 412749. https://doi.org/10.1016/J.PHYSB.2020.412749.

[244] K. Toda, R. Furue, S. Hayami, Recent progress in applications of graphene oxide for gas sensing: A review, Anal. Chim. Acta. 878 (2015) 43–53. https://doi.org/10.1016/J.ACA.2015.02.002.

[245] B. Cai, L. Huang, H. Zhang, Z. Sun, Z. Zhang, G.J. Zhang, Gold nanoparticles-decorated graphene field-effect transistor biosensor for femtomolar MicroRNA detection, Biosens. Bioelectron. 74 (2015) 329–334. https://doi.org/10.1016/J.BIOS.2015.06.068.

[246] K. Ganesan, V.K. Jothi, A. Natarajan, A. Rajaram, S. Ravichandran, S. Ramalingam, Green synthesis of Copper oxide nanoparticles decorated with graphene oxide for anticancer activity and catalytic applications, Arab. J. Chem. 13 (2020) 6802–6814. https://doi.org/10.1016/J.ARABJC.2020.06.033.

[247] N.F. Rosli, M. Fojtů, A.C. Fisher, M. Pumera, Graphene Oxide Nanoplatelets Potentiate Anticancer Effect of Cisplatin in Human Lung Cancer Cells, Langmuir. 35 (2019) 3176–3182. https://doi.org/10.1021/acs.langmuir.8b03086.

[248] N. Ma, J. Liu, W. He, Z. Li, Y. Luan, Y. Song, S. Garg, Folic acid-grafted bovine serum albumin decorated graphene oxide: An efficient drug carrier for targeted cancer therapy, J. Colloid Interface Sci. 490 (2017) 598–607. https://doi.org/10.1016/j.jcis.2016.11.097.

[249] J. Tian, Y. Luo, L. Huang, Y. Feng, H. Ju, B.Y. Yu, Pegylated folate and peptide-decorated graphene oxide nanovehicle for in vivo targeted delivery of anticancer drugs and therapeutic self-monitoring, Biosens. Bioelectron. 80 (2016) 519–524. https://doi.org/10.1016/j.bios.2016.02.018.

[250] S. Javanbakht, H. Namazi, Doxorubicin loaded carboxymethyl cellulose/graphene

quantum dot nanocomposite hydrogel films as a potential anticancer drug delivery system, Mater. Sci. Eng. C. 87 (2018) 50–59. https://doi.org/10.1016/j.msec.2018.02.010.

[251] N. Karki, H. Tiwari, M. Pal, A. Chaurasia, R. Bal, P. Joshi, N.G. Sahoo, Functionalized graphene oxides for drug loading, release and delivery of poorly water soluble anticancer drug: A comparative study, Colloids Surfaces B Biointerfaces. 169 (2018) 265–272. https://doi.org/10.1016/j.colsurfb.2018.05.022.

[252] Q. Yang, X. Pan, F. Huang, K. Li, Fabrication of High-Concentration and Stable Aqueous Suspensions of Graphene Nanosheets by Noncovalent Functionalization with Lignin and Cellulose Derivatives, (n.d.). https://doi.org/10.1021/jp910232x.

[253] S. Hou, S. Su, M.L. Kasner, P. Shah, K. Patel, C.J. Madarang, Formation of highly stable dispersions of silane-functionalized reduced graphene oxide, Chem. Phys. Lett. 501 (2010) 68–74. https://doi.org/10.1016/J.CPLETT.2010.10.051.

[254] L. Guardia, M.J. Ferná Ndez-Merino, J.I. Paredes, P. Solís-Ferná Ndez, S. Villar-Rodil, A. Martínez-Alonso, J.M.D. Tascó, High-throughput production of pristine graphene in an aqueous dispersion assisted by non-ionic surfactants, Carbon N. Y. 49 (2011) 1653–1662. https://doi.org/10.1016/j.carbon.2010.12.049.

[255] S. Wang, M. Yi, Z. Shen, The effect of surfactants and their concentration on the liquid exfoliation of graphene, RSC Adv. 6 (2016) 56705–56710. https://doi.org/10.1039/C6RA10933K.

[256] D. Li, M.B. Müller, S. Gilje, R.B. Kaner, G.G. Wallace, Processable aqueous dispersions of graphene nanosheets, Nat. Nanotechnol. 2008 32. 3 (2008) 101–105. https://doi.org/10.1038/nnano.2007.451.

[257] S. Kashyap, S. Mishra, S.K. Behera, Aqueous Colloidal Stability of Graphene Oxide and

Chemically Converted Graphene, J. Nanoparticles. 2014 (2014) 1–6. https://doi.org/10.1155/2014/640281.

[258] J. Taha-Tijerina, D. Venkataramani, C.P. Aichele, C.S. Tiwary, J.E. Smay, A. Mathkar, P. Chang, P.M. Ajayan, Quantification of the Particle Size and Stability of Graphene Oxide in a Variety of Solvents, Part. Part. Syst. Charact. 32 (2015) 334–339. https://doi.org/10.1002/PPSC.201400099.

[259] H. Zhang, S. Wang, Y. Lin, M. Feng, Q. Wu, Stability, thermal conductivity, and rheological properties of controlled reduced graphene oxide dispersed nanofluids, Appl. Therm. Eng. 119 (2017) 132–139. https://doi.org/10.1016/j.applthermaleng.2017.03.064.

[260] Z. Xia, G. Maccaferri, C. Zanardi, M. Christian, L. Ortolani, V. Morandi, V. Bellani, A. Kovtun, S. Dell'Elce, A. Candini, A. Liscio, V. Palermo, Dispersion Stability and Surface Morphology Study of Electrochemically Exfoliated Bilayer Graphene Oxide, J. Phys. Chem. C. 123 (2019) 15122–15130. https://doi.org/10.1021/ACS.JPCC.9B03395

Table 1. Physico-chemical properties of GBN

Properties	**Graphene**	**rGO**	**GO**
Mechanical properties	Stiffness: 340 $N \cdot m^{-1}$ [219]; Young's modulus: 1.0 ± 0.1TPa [219]; strength: 42 $N \cdot m^{-1}$ (130 GPa) [219].	Stiffness: 22.4 $N \cdot m^{-1}$[220]; Young's modulus: 0.25± 0.15 TPa [221]; strength: 293.3 MPa [222].	Stiffness: 145.3 $N \cdot m^{-1}$ [223]; Young's modulus: 207.6 ± 23.4 GPa [223]; strength: 17.3 $N \cdot m^{-1}$ (24.7 GPa) [224].
Electrical properties	Electrical conductivity: 6500 $S \cdot m^{-1}$ [225]; electron mobility: 25 $m^2 V^{-1} s^{-1}$ [226]; sheet resistance: 30 Ω per square of 2D area (30 Ω/sq) at 97.7 % transmittance [226].	Electrical conductivity: 3032.6-4006 $S \cdot m^{-1}$ [227]; electron mobility: 26 $cm^2 V^{-1} s^{-1}$ [228]; sheet resistance: 1.6 KΩ /sq at 85% transparency [229].	Electrical conductivity: $1.34 \cdot 10^{-5}$ $S \cdot m^{-1}$ [230]; electron mobility: 2-200 $cm^2 V^{-1} s^{-1}$ [231]; sheet resistance: 276-2024 Ω/sq at 23–77% transparency [232].
Thermal properties	Thermal conductivity: ranges from	Thermal conductivity: 1.3	Thermal conductivity: 8.8

	(1500-5000) $W \cdot m^{-1} \cdot K^{-1}$[233].	$W \cdot m^{-1} \cdot K^{-1}$[234].	$W \cdot m^{-1} \cdot K^{-1}$ [235].
Application	Biomedicine [236], energy [156], electronics [237], nanocomposites [238], nanosensors [226].	Biomedicine [239], energy [240], electronics [241], nanocomposites [238], nanosensors [242].	Biomedicine [158], energy [243], nanocomposites [238], nanosensors [244].

Table 2. Applications, properties and description of key results of nanocomposite materials.

GBN-nanocomposite type and composition information	**Application**	**Key results and description**	**Reference**
GO- AgNp Characteristics of nanocomposite: -GO thickness: 0.7-1.2 nm; -distribution size: 300-800 nm. -AgNps size: 7.5 nm.	Antibacterial agent. Antibacterial coatings for preventing growth of bacteria on medical devices.	Inhibitory concentration of GO-AgNp towards *Pseudomonas aeruginosa* is 2.5 $\mu g \cdot ml^{-1}$ with 100% inhibition rate after 1 h. In the case of GO the authors did not observe antibacterial activity. Role of GO: (*i*) stabilizing agent preventing agglomeration of AgNp; (*ii*) increasing of surface area of AgNps.	[120]
GO-TETA-AgNps Characteristics of nanocomposite: -GO covalently functionalised with N-(trimethoxysilylpropyl) ethylenediaminetriacetic acid trisodium salt (TETA) and	Sensors for organic molecules (*p* -aminothiophenol and melamine). Antibacterial agents.	Detection limit for *p*-aminothiophenol- $2 \cdot 10^{-8}$ M and melamine- $2 \cdot 10^{-7}$ M. Inhibition effect (100%) against the growth of *Escherichia coli* (*E. coli*) at *C (*GO-TETA-Ag)= 100 $\mu g \cdot ml^{-1}$.	[123]

AgNps (30-50 nm); -stable aqueous dispersion at *C* (GO-TETA-AgNps)=0.5 $mg \cdot ml^{-1}$. -uniform distribution of AgNps on graphene surface (according to SEM).			
rGO-PDA-AgNps Characteristics of nanocomposite: -rGO modified with polydopamine-AgNps; -heterogeneous distribution of AgNps on graphene surface with non-uniform sizes leading to increasing immobilization of	DNA biosensors.	Detection limit of $3.2 \cdot 10^{-15}$ M. Application of rGO allows to increase electrode active area and enhance detection signal.	[126]

the target molecules.			
rGO-1,6 diaminohexane-AgNp. Characteristics of nanocomposite: -rGO noncovalently functionalised with 1,6 diaminohexane- AgNp (by hydrogen bonding, electrostatic interactions); -using of single layers of graphene sheets (according to HRTEM) leads to homogeneous distribution of AgNps.	Antibacterial activity, water disinfection.	Disinfecting water against total and fecal coliform bacteria at C= 1 mg·ml^{-1} with 100 % inhibition rate.	[45]
rGO-AuNps-PNA	Biosensors for	Detection limit up to 1·10^{-14} M. In the absence of AuNps	[245]

Characteristics of nanocomposite: -rGO noncovalently modified with AuNps which in turn covalently functionalised with peptide nucleic acid probe (PNA); -the sequence of the PNA probe is N-AACCACACAACCTACTACCTCA-C; -rGO thickness: 1.6 nm; -particle size of AuNps: 10 nm.	miRNA.	detection limit is equal to $1 \cdot 10^{-13}$M.	
rGO-AuNps-TGA Characteristics of nanocomposite:	Sensors for detection of mercury (II) ions.	Detection limit up to $2.5 \cdot 10^{-8}$ M.	[131]

-noncovalently functionalised rGO with AuNps followed by covalent functionalisation with thioglycolic acid (TGA); -homogenious distribution of AuNps (5 nm) on rGO surface without agglomerations.			
rGO-PtNps Characteristics of nanocomposite: -superior dispersion of PtNps on rGO surface; -small particle size of rGO-PtNps: 1.9 nm; surface area: 138 $m^2 \cdot g$; PtNps loading: 0.25 mg cm^{-2}.	Fuel cells.	High fuel cell performance of rGO-PtNps with maximum power output of 320 $mW \cdot cm^{-2}$ (40% higher than for carbon black (Vulcan XC-72) modified with PtNps (Pt-VC)). The high fuel cell performance using low loading of PtNps (0.25 mg cm^{-2}) in comparison to higher Pt loading used in standard fuel cell electrodes (0.5 mg cm^{-2}). High fuel cell performance is referred to high catalytic activity due to high electrochemical surface area and small PtNps size.	[140]

rGO-T-Pt Characteristics of nanocomposite: - rGO-taurine-PtNp; -rGO modified with taurine and PtNps; -thickness of rGO-T is 1.2 nm with lateral dimensions of several micrometers; -loading of Pt up to 80 wt%.	Electrocatalyst for methanol oxidation. Fuel cells.	Higher electrocatalytic activity than Pt-VC and Pt-rGO catalysts. Electrode charge transfer resistance R_{ct} =158, 185 and 203 Ω for rGO-T-Pt, rGO-Pt and Pt-VC, respectively. Catalytic enhancement mechanism of rGO-T-Pt: (*i*) presence of SO_3H^- groups due to functionalisation of rGO with taurine molecules; (*ii*) uniform and symmetrical distribution of PtNps with particle size of 3.8 nm on rGO –T surface; (*iii*) enhanced charge transfer ability.	[142]
rGO-ZnO Characteristics of nanocomposite: -ZnO particle diameter: 20 ± 2 nm; -lateral size dimensions of rGO	Sensors for NO_2.	rGO-ZnO sensor has higher response than ZnO sensor toward NO_2 gas at 200 ^{0}C and 250 ^{0}C. Response of the sensor rGO-ZnO to NO_2 gas at C (NO_2) = 5 ppm is 1.4 times higher than that of pure ZnO sensor.	[144]

sheets range from few nanometers up to some tens of micrometers.			
G-ZnO-PSE-ssDNA Characteristics of nanocomposite: -graphene-ZnO -single stranded DNA; -noncovalent composite of graphene (G)-ZnO- 1-pyrenebutyric acid N-hydroxysuccinimide ester (PSE) that was covalently functionalised with amino modified ssDNA probe; -ssDNA probe was used to	Genosensors for ss RNA detection.	Detection limit is $4.3 \cdot 10^{-12}$ M due to high conductivity of G-ZnO (R_{ct} =1241.3 Ω.), large specific area and catalytic properties.	[143]

hybridize with ssRNA target for detection.			
GO- CuO Characteristics of nanocomposite: -CuO loading: 40%; -thickness of GO layers is 12 nm; -thickness of GO-CuO layers is 13 nm; -particle size of CuO is190 nm.	Antibacterial agent.	Inhibiting the growth of *E. coli* and *S. typhimurium* bacteria in the concentration range 1-3 $mg \cdot ml^{-1}$, toxicicty for both bacteria after 3 h is 98% at *C* (GO-CuO)= 3 $mg \cdot ml^{-1}$. Mechanism of antibacterial activity: (*i*) cellular uptake, (*ii*) generation of reactive oxygen species.	[148]
GO-CuO Characteristics of nanocomposite: -agglomerated CuO nanoparticles with spherical	Anticancer activity. Photocatalyst for dye degradation.	Cytotoxic activity (70%) against Human colon cancer cell line (HCT-116) at 100 $\mu g \cdot ml^{-1}$. GO-CuO led to 83.20 % degradation of methylene blue dye solution when exposed to visible light for 60 min (due to generation of $^{\bullet}OH$ and $^{\bullet}O_2^-$radicals that oxidize methylene	[246]

morphology.		blue).	
rGO-Fe_3O_4 Characteristics of nanocomposite: -Fe_3O_4 particle size: 6 ±3nm; -superparamagnetic properties: saturation magnetisation (Ms = 20.1 emu·g^{-1}) and coercivity (Hc=6.25 Oe).	Anticancer agents. Antibacterial agents.	Anticancer activity: cytotoxicity of rGO-Fe_3O_4 against erythromyeloblastoid leukemia (K562), prostate carcinoma (PC-3), epidermoid carcinoma (A-431), ER^+ breast carcinoma (MDA-MB-231), colon carcinoma (COLO-205), ER1 breast adenocarcinoma (MCF-7), and lung carcinoma (A-549) cell lines at *C* (rGO-Fe_3O_4)=50 μg·ml^{-1} is equal to 20–40% depending on cell line Antibacterial activity: minimum inhibitory concentration of rGO-Fe_3O_4= 1000 μg·ml^{-1} against Gram-positive bacteria, (*Staphylococcus aureus*, *Bacillus subtilis*, *Streptococcus mutans*, and *Enterococcus faecalis*) and Gram-negative bacteria (*Salmonella typhi* and *E. coli).*	[150]
GO–APTES-Fe_3O_4 -DOX Characteristics of nanocomposite:	Targeted drug delivery. Dual *in-vitro* fluorescence	Targeted delivery of DOX with loading capacity of 0.2 mg of DOX per 1 mg GO-Fe_3O_4-APTES (20 wt % loading). DOX- GO-Fe_3O_4-APTES led to 2.5 fold higher efficacy of	[154]

-GO covalently functionalised with 3–aminopropyltriethoxysilane (APTES) and noncovalently with Fe_3O_4 and DOX; -particle size of GO-Fe_3O_4-APTES: 260 nm.	and *in-vivo* magnetic resonance imaging. Cancer sensing.	cytotoxicicty (62%) against HeLa cells than free DOX (reducing the required dose of DOX by 8 times to have the same value of cytotoxicity). The intensity ratio of emission spectra of GO-Fe_3O_4-APTES in red (635 nm) and green (535 nm) for cancer (HeLa and MCF-7) and healthy cell line (HEK-293) depends on the type of cell line and its pH value in the cell microenvironment.	

Table 3. Cytotoxicity of conjugates based on GBN and non-covalently attached anticancer drugs evaluated by cell viability assay.

Type of GBN	**Drug load**	**Cell lines or type of cancer**	**Applied concentrations and *IC_{50}* or approximate % of cytotoxicity at the highest concentration**	**Reference**
GO-sulphonic acid groups- folic acid (GO-SO_3H-FA); GO-FA	Loading of a dual drug: camptothecin (CPT) (4.5 %) and Dox (400%).	MCF-7 cells (human breast adenocarcinoma)	C= 2 and 20 $\mu g \cdot ml^{-1}$ for (GO-SO_3H-DOX-FA), % cytotoxicity = 20% and for GO-FA-DOX (% cytotoxicity = 67%) C= 0.002, 0.02 and 0.2 $\mu g \cdot ml^{-1}$ for (GO-FA-DOX-CPT) of % cytotoxicity = 22% and (GO-FA-CPT) % cytotoxicity: = 26%	[168]
GO- chlorotoxin (GO-CTX)	Loading of DOX 570 mg DOX per gm GO-CTX.	C6 (glioma cells)	C= 1-5 $\mu g \cdot ml^{-1}$; % of cytotoxicity = 60%	[104]
GO-sodium alginate (GO-SA)	Loading of DOX 1.8 mg/mg.	HeLa cells	C= 5 - 20 $\mu g \cdot ml^{-1}$ % of cytotoxicity = 69%	[169]
GONP with dimensions of 50 × 50 nm^2	Cisplatin (CP) loading was not determined.	A549 (human lung cancer cell line)	C= 2.5 – 30 $\mu g \cdot ml^{-1}$ % of cytotoxicity = 90%	[247]
GO-polyethylene glycol-folic acid (GO-PEG-FA)	Camptothecin (CPT) loading 45%.	MCF-7 (breast cancer cell line)	C= 20 – 100 $\mu g \cdot ml^{-1}$ % of cytotoxicity = 76%	[173]

GO-Fe_3O_4-β-cyclodextrin	DOX loading 37.4 % MTX loading 23.4 %	K562 cells (leukemia cell line)	C= 2 – 16 μg·ml^{-1} % of cytotoxicity (DOX) = 65% % of cytotoxicity (MTX) = 55%	[174]
GO-PEG-FA	Loading of Protocatechuic acid (PCA)- 23.47% and Chlorogenic acid (CA)- 18.33%.	HT29 (Colon cancer cell line); HePG2 (human liver cancer cell line)	C= 1.56 – 100 μg·ml^{-1} % of cytotoxicity (HT29) = 58% IC_{50} (HT29) = 50.69 μg·ml^{-1}; % of cytotoxicity (HepG2)= 61% IC_{50} (HepG2) = 40.39 μg·ml^{-1}	[177]
GO-FA- bovine serum albumin (GO-FA-BSA)	DOX Loading- 437.43 μg DOX / mg (GO-FA-BSA).	MCF-7 (human breast cancer cell line) FA-receptor-positive) A549 (human lung cancer cell line) (FA-receptor-negative)	C= 0.01– 20 μg·ml^{-1} IC_{50} (MCF-7, 24 h) = 8.9 ± 0.7 μg·ml^{-1} IC_{50} (MCF-7, 48 h) = 0.048 ± 0.010 μg·ml^{-1} (% of cytotoxicity = 83%) IC_{50} (A549, 24 h) = 5.3 ± 0.7 μg·ml^{-1} IC_{50} (A549, 48 h) = 0.279 ± 0.037 μg·ml^{-1} (% of cytotoxicity = 78%)	[248]
FA–GO–PVP (folic acid-GO-polyvinylpyrrolidone, M= 30kDa)	DOX loading -107.5 %.	HeLa cells	2 μg·ml^{-1}; 20 μg·ml^{-1} (% of cytotoxicity = 71%)	[170]

Fluorinated GO (FGO)	loading of DOX ~200%	HeLa cells	C= 1.11 – 30 $\mu g \cdot ml^{-1}$ (% of cytotoxicity (24 h) = 70%) (% of cytotoxicity (48 h) = 94%)	[179]
Pegylated folate and peptide-decorated graphene oxide PEG-FA-Pep-GO	CPT loading- 90%	HeLa cells	IC_{50} = 3.1 μM	[249]
Graphene quantum dots - carboxymethyl cellulose hydrogel (GQD - CMC)	DOX loading is dose dependent on GQD GQD(10%)-CMC ~ 4.5%, GQD(20%)-CMC ~5.5 % GQD(30%)-CMC~6 %	blood cancer cells (K562)	C= 2- 32 $\mu g \cdot ml^{-1}$ With IC_{50} values of 5.1 $\mu g \cdot ml^{-1}$ GQD (% cytotoxicity = 93%)	[250]
GO-PVP and GO- β-cyclodextrin (CD)	The anticancer drug SN-38 (7-ethyl-10-hydroxy camptothecin) The loading:- 1 g of GO-PVP loaded 0.17 g of SN-38 ; 1 g of GO-β-CD loaded 0.14 g of SN-38	MCF-7	5 and 10 $\mu g \cdot ml^{-1}$ IC_{50}(GO-PVP-SN-38) =97 μM (% cytotoxicity = 68%) IC_{50}(GO-β-CD-SN-38) = 170 μM (% cytotoxicity = 65%)	[251]

Table 4. Characteristics of GBN dispersions

System	Mechanism of dispersion stabilization	Characteristics of dispersion	Category of stabilization process	Reference
GO covalently functionalised by SO_3H groups (GO-SO_3H).	The presence of negatively charged HSO_3^- functional groups on GO surface cause electrostatic repulsion of the graphene layers.	Duration of stability investigation: one month. C(GO-SO_3H)=2 mg·ml^{-1}. pH range: 3-10. ζ-potential: -55-60 mV at pH 6.	Functionalisation	[213]
Graphene noncovalently functionalised with tetrapotassium salt of coronene tetracarboxylic acid (G-CS) Graphene was obtained by two methods: thermal exfoliation of graphite oxide and the arc evaporation of	The negatively charged CS molecules form noncovalent π-π stacking interactions with graphene surface and prevent π-π stacking interactions between graphene layers stabilising the	Duration of stability investigation: months. C(G-CS)=0.15 mg·ml^{-1}.	Functionalisation	[54]

graphite in a hydrogen atmosphere.	dispersions of G-CS.			
Graphene functionalised with hydroxyl groups (G-OH).	(*i*) presence of oxygen containing groups; (*ii*) high negative charge density of the graphene surface.	Duration of stability investigation: one month. *C*(G-OH)=0.1-5 mg·ml^{-1}. ζ-potential: -50mV.	Functionalisation	[211]
Graphene-SiO_2.	(*i*) increased hydrophilicity due to the presence of SiO_2 groups;. (*ii*) steric hinderance effect provided by the SiO_2 groups.	Duration of stability investigation: 7 days.	Functionalisation	[217]
rGO non covalently functionalised with natural polymers: sodium lignosulfonate (SLS, M_w=60000), sodium carboxymethyl cellulose (SCMC, M_w=250000), and pyrene-containing	rGO +SLS: (*i*) hydrophobic interaction of alkyl groups and aromatic rings of SLS with graphene surface through π-π stacking interaction; (*ii*) the	Duration of stability investigation: four months. *C*(rGO-polymer)=0.6-2 mg·ml^{-1}.	Functionalisation	[252]

hydroxypropyl cellulose (HPC-Py).	sulphonic groups ($-SO_3Na$) provide sufficient electrostatic repulsion. rGO + SCMC: electrostatic repulsion of carboxylate anions. rGO + HPC-Py: steric repulsion caused by the long polymer chains.			
rGO covalently functionalised with N-(trimethoxysilylpropyl) ethylenediamine triacetic acid (NEDTA).	The hydrophilic EDTA groups stabilized rGO-NEDTA aqueous dispersions.	Duration of stability investigation: three months. *C*(rGO-NEDTA)=1 $mg \cdot ml^{-1}$.	Functionalisation	[253]
Graphene + sodium dodecylbenzene sulfonate (SDBS).	the aqueous dispersions were stabilised by Coulomb repulsion	Duration of stability investigation: 6 weeks.	Surfactant addition	[215]

The graphene was obtained by ultrasound exfoliation of graphite in water solution of SDBS surfactant. The final nanomaterial contained 40 % of multilayered graphene (< 5 layers), 3% monolayered.	between the G-SDBS sheets.	Particle size: 500 nm. *C*(G-SDBS)=0.5mg·ml^{-1}. ζ-potential: -50 mV at pH=7.		
Graphene + ionic and nonionic surfactants [P123, Tween 80, Triton X-100, polyvinylpyrrolidone, poly(sodium 4-styrenesulfonate), sodium deoxycholate, sodium dodecylbenzene-sulfonate, 1-pyrenebutyric acid, sodium dodecyl sulphate, sodium taurodeoxycholate hydrate, hexadecyltrimethylammonium bromide].	Addition of ionic and nonionic surfactants maintained exfoliation between graphene layers through electrostatic repulsion forces.	Duration of stability investigation: one month. Size of graphene flakes: several hundred nanometers *C*(G-surfactant)=1 mg ml^{-1}.	Surfactant addition	[254,255]

Graphene + sodium cholate (G-SC).	Addition of amphiphilic surfactant provides π-π stacking interaction with graphene surface (through hydrophobic domains) and stabilisation in water (through hydrophilic domains). At the same time the electrostatic repulsion between G-SC layers takes place due to the presence of negatively charged cholate ions on the graphene surface.	Duration of stability investigation: one week C(G-SC)=11 mg·l^{-1} ζ-potential: -45 mV.	Surfactant addition	[216]
Graphene + anionic surfactant sodium dodecyl benzene sulfonate (SDBS).	G-SDBS dispersions stabilized by the electrostatic repulsion caused by addition of SDBS that increases the charge density of	Duration of stability investigation: one week.	Surfactant addition	[217]

	graphene surface.			
Chemically converted graphene (CCG) (synthesized by GO reduction by hydrazine hydrate without total conversion of all oxygen-containing functional groups and remaining of few COOH groups).	The presence of carboxylate ions on CCG-surface increases the electrostatic repulsion between graphene layers.	Particle size: 200 – 1000 nm. *C*(CCG)=0.05 mg·ml^{-1}. ζ-potential is pH dependent: -30 to -43 mV in the pH range 6.1 to 10.	Exfoliation	[256,257]
GO	Electrostatic repulsion between GO layers due to presence of oxygen containing functional groups (C-OH and COOH). pH can affect the stability of colloids due to changing the charge of nanoparticles in the following processes: (*i*) protonation of acidic groups (C-	Particle size: 200 – 1000 nm. Highest ζ-potential −48.6 mV at pH 10. The dispersions are stable of pH= 4-11.	Exfoliation	[257]

	OH and COOH) in acidic medium (*ii*) deprotonation of C-OH and COOH groups in alkaline medium leading to increase of negative charge and electrostatic repulsion.			
GO + ethylene glycol (EG); GO + deionized water (DW); GO + ethanol (E); GO + mineral oil (MO).	High polarity of the solvents (EG, DW and E) leads to high ζ-potential values of GO; nonpolar solvent (MO) leads to low ζ-potential values of GO and hence decrease the stability of dispersions.	Particle sizes (μm): 0.11 (GO-DW), 22.23 (GO-EG), 0.33 (GO-E), 0.90 (GO-MO). *C*(GO)=0.2 wt%. ζ-potentials (mV): -113.77 (GO-DW), 4037.1 (GO-EG), -39.1 (GO-E), 6.60 (GO-MO).	Exfoliation	[258]
rGO	Due to presence of residual	Duration of stability	Exfoliation	[259]

	hydrophilic groups after GO reduction such as hydroxyl, carboxyl, and carbonyl groups.	investigation: 15 days without sedimentations while the authors observed sedimentation after 45 days *C*(rGO)=0.2 mg·ml^{-1}. ζ-potential: -50.9 mV at pH 12.		
GO + polar solvents (water, methanol, ethanol, DMF, THF).	Electrostatic repulsion forces due to the presence of oxygen containing groups on GO surface (hydroxyl and carboxyl) that stabilize graphene dispersions due to increasing of charge density.	Duration of stability investigation: two months. Size of particles: 1-10 μm. *C*(GO)=0.33 mg·ml^{-1}. ζ-potential: −25 to −46 mV depending on solvent type.	Exfoliation	[260]

List of abbreviations

ADP	Adenosine diphosphate
AD	Adipic acid dihydrazide
Arg	Arginine
APTS	3- Aminopropyltriethoxysilane
B	Benzene
BT	Benzothiophene
CVD	Chemical vapor deposition
CCG	Chemically converted graphene
DW	Deionized water
DBT	Dibenzothiophene
EDC	1-(3-Dimethylaminopropyl)-3-ethylcarbodiimide
DMF	Dimethyl formamide
E	Ethanol
EDTA	Ethylenediamine triacetic acid
EG	Ethylene glycol
GO-SO_3H	GO covalently functionalised by SO_3H groups
EOGO	GO, enriched by oxygen containing groups
GFC	GO functionalised with L-cysteine
GFM	GO functionalised with L-methionine
GBN	Graphene based nanomaterials (GO, rGO, graphene)
G-OH	Graphene functionalized with hydroxyl groups
G-CS	Graphene noncovalently functionalised with tetrapotassium salt of

	coronene tetracarboxylic acid
G-epitaxial	Graphene obtained by epitaxial growth method
GO	Graphene oxide
GrO	Graphite oxide
HSA	Human serum albumin
HA	Hyaluronic acid
Lys	Lysine
Man-GO	Mannosylated ethylenediamine GO
MO	Mineral oil
(NHC-Pd^{2+})	N-heterocyclic carbene–palladium complex
NHS	N-Hydroxysuccinimide
DCC	N,N′-Dicyclohexylcarbodiimide
NEDTA	N-(trimethoxysilylpropyl) ethylenediamine triacetic acid
PEG	Polyethylene glycol
HPC-Py	Pyrene-containing hydroxypropyl cellulose
P	Pyridine
rGO	Reduced graphene oxide
SCMC	Sodium carboxymethyl cellulose
SC	Sodium cholate
SDBS	Sodium dodecylbenzene sulfonate
SLS	Sodium lignosulfonate
THF	Tetrahydrofuran
TRGO	Thermally reduced graphene oxide

T	Thiophene

Cell lines

K562	Blood cancer
MCF-7	Breast cancer
HT29	Colon cancer
COLO-205	Colon carcinoma
A-431	Epidermoid carcinoma
MCF-7	ER1 breast adenocarcinoma
MDA-MB-231	ER^+ breast carcinoma
K562	Erythromyeloblastoid leukemia
C6	Glioma
MCF-7	Human breast adenocarcinoma
MCF-7	Human breast cancer
KB	Human carcinoma
HeLa	Human cervical carcinoma
HCT-116	Human colon cancer
HEK293	Human embryonic kidney 293
HePG2	Human liver cancer
A549	Human lung cancer
HLF	Human lung fibroblast
hMSCs	Human mesenchymal stem
RPMI 8226	Human multiple myeloma
Cal-27	Human squamous cell carcinoma

K562	Leukemia
A-549	Lung carcinoma
PA-1	Ovarian cancer
PC-3	Prostate carcinoma
rADSCs	Rat adipose tissue-derived stromal

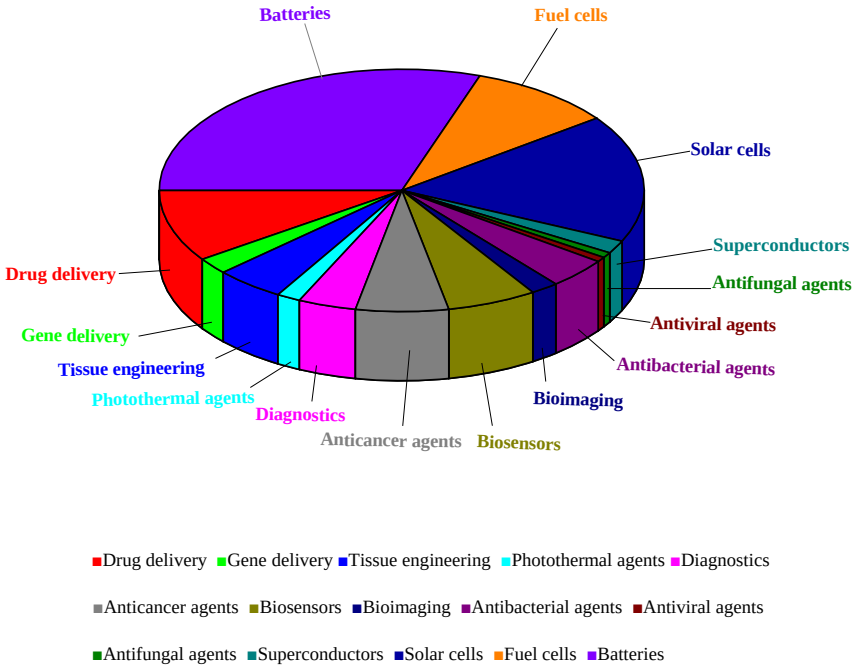

Fig. 1. Publication distribution of GBN applications in various research areas.

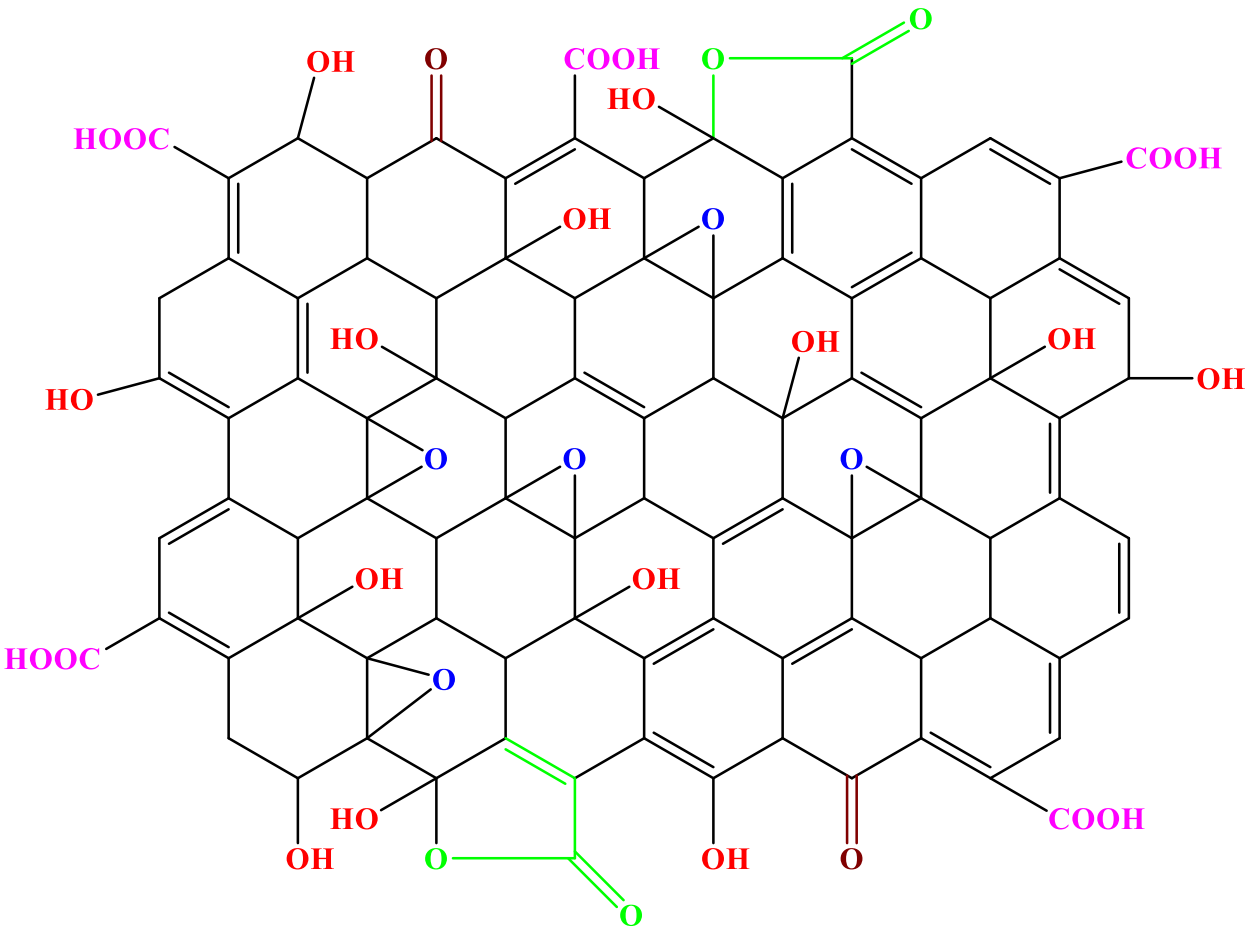

Fig. 2. GO structure

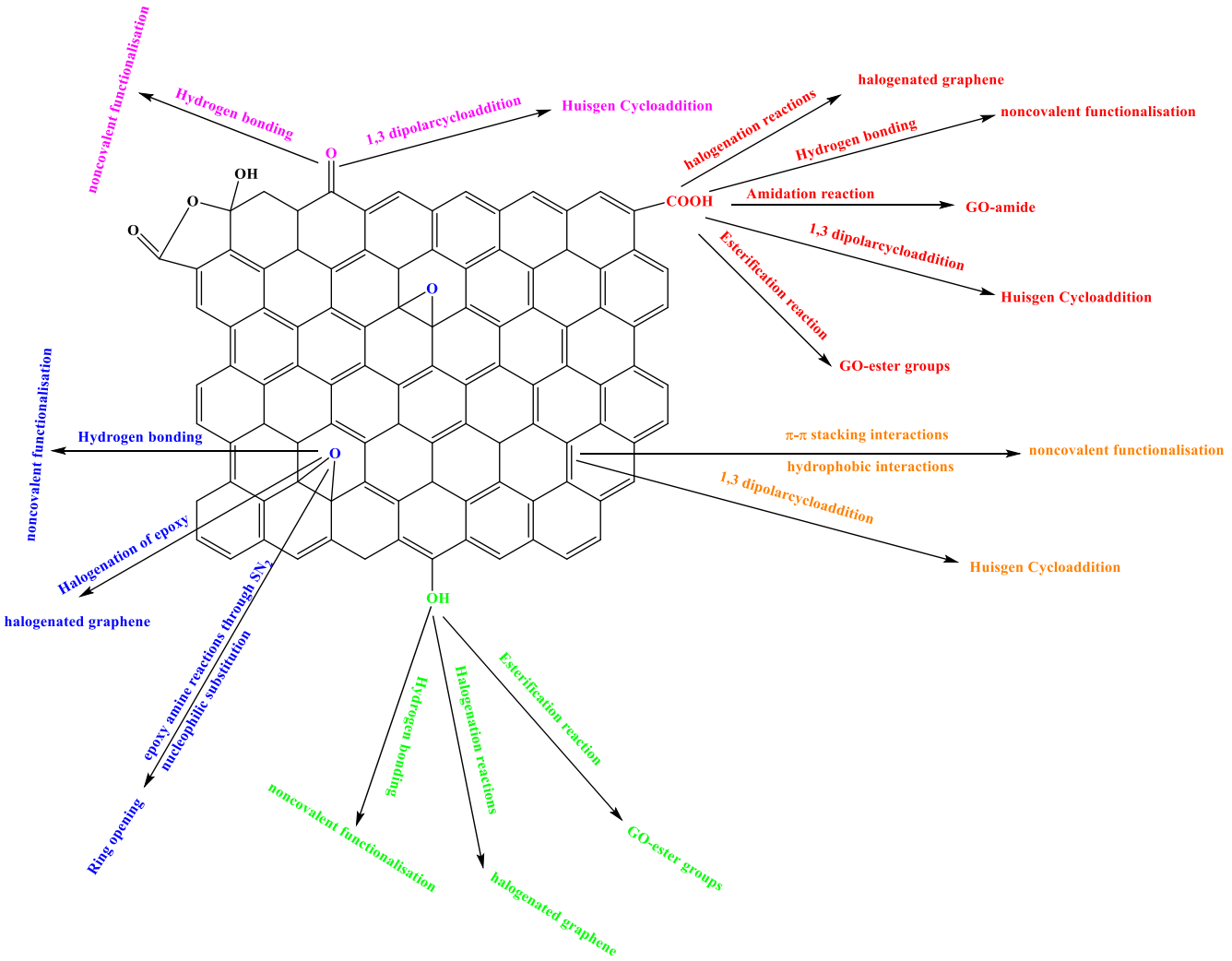

Fig. 3. Scheme showing various kinds of reactions that can happen on the graphene surface.

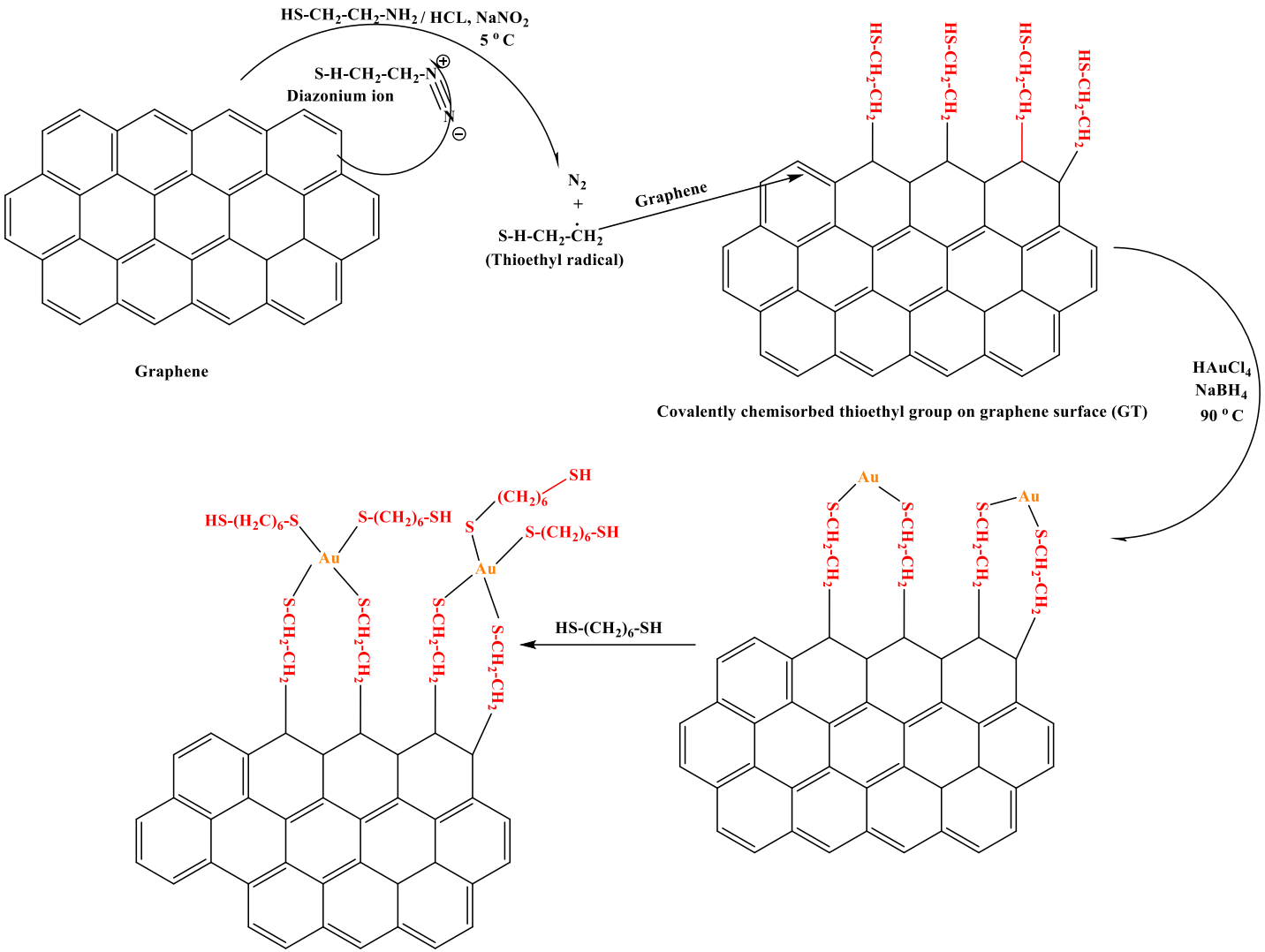

Fig. 4. Schematic of the reaction mechanism for spontaneous reduction of thioethyldiazonium ($HS\text{-}C_2H_4NN^+$) ions on graphene surface with subsequent covalent immobilisation of AuNPs on graphene followed by the reaction with dithiol molecules [111].

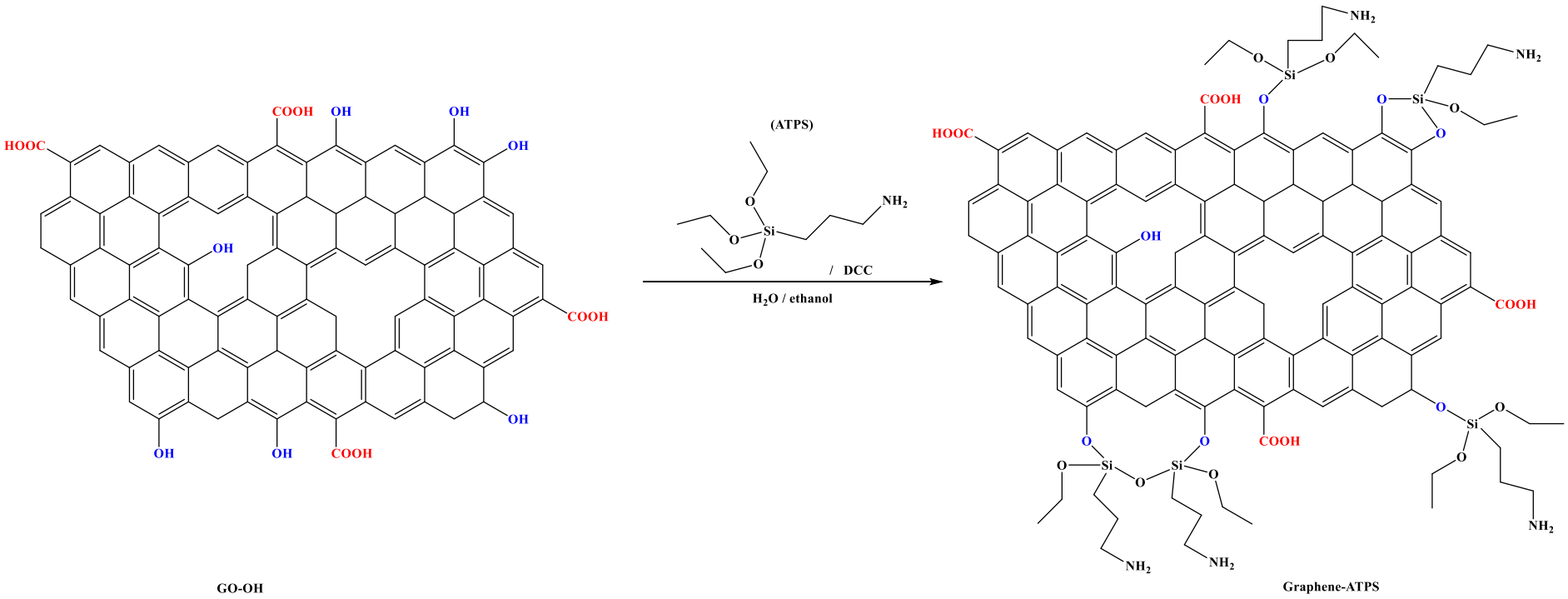

Fig. 5. Functionalisation of hydroxyl groups of GO with APTS through covalent bonding [112].

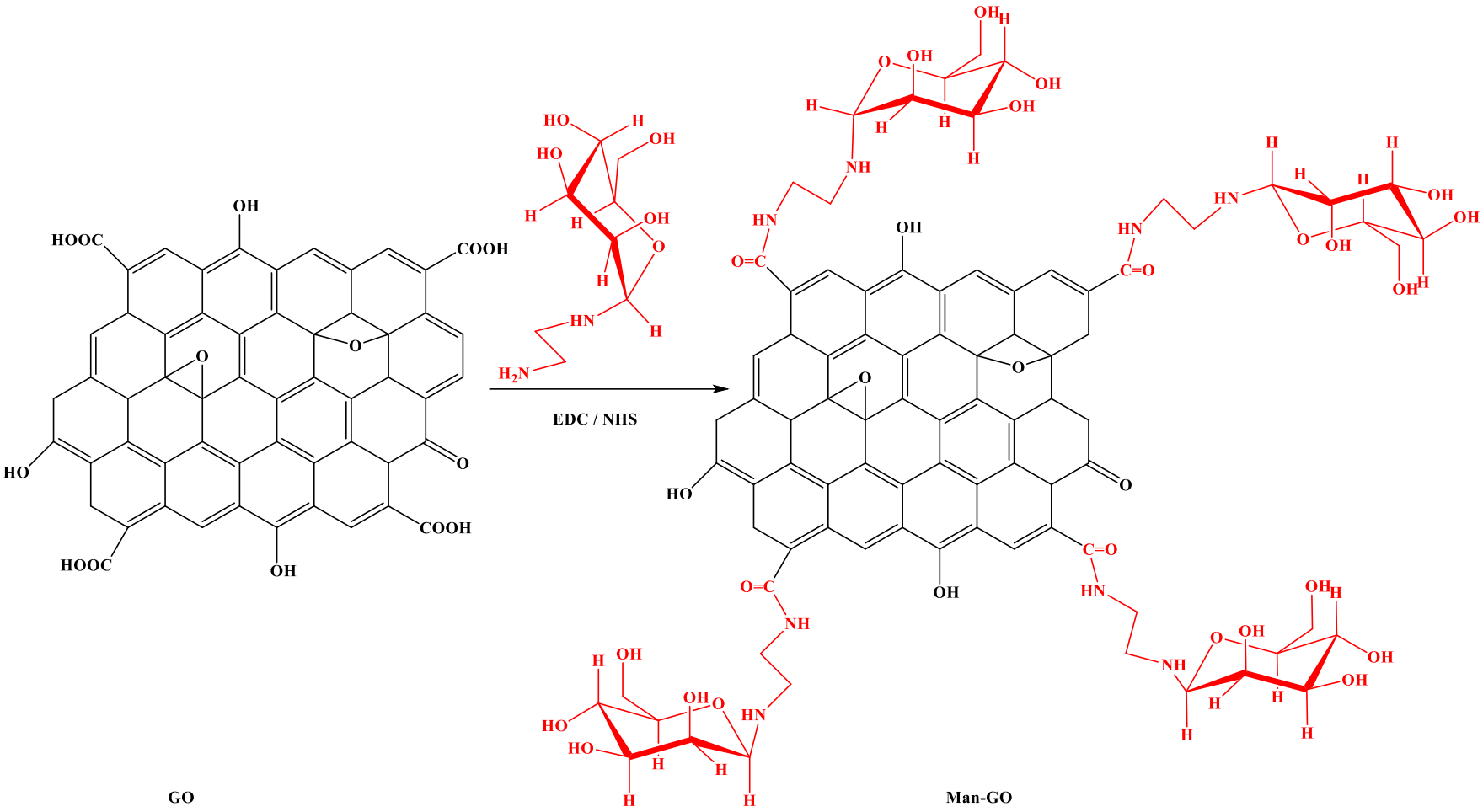

Fig. 6. Covalent functionalisation of GO with mannosylated ethylenediamine (in red) through EDC / NHS coupling [113].

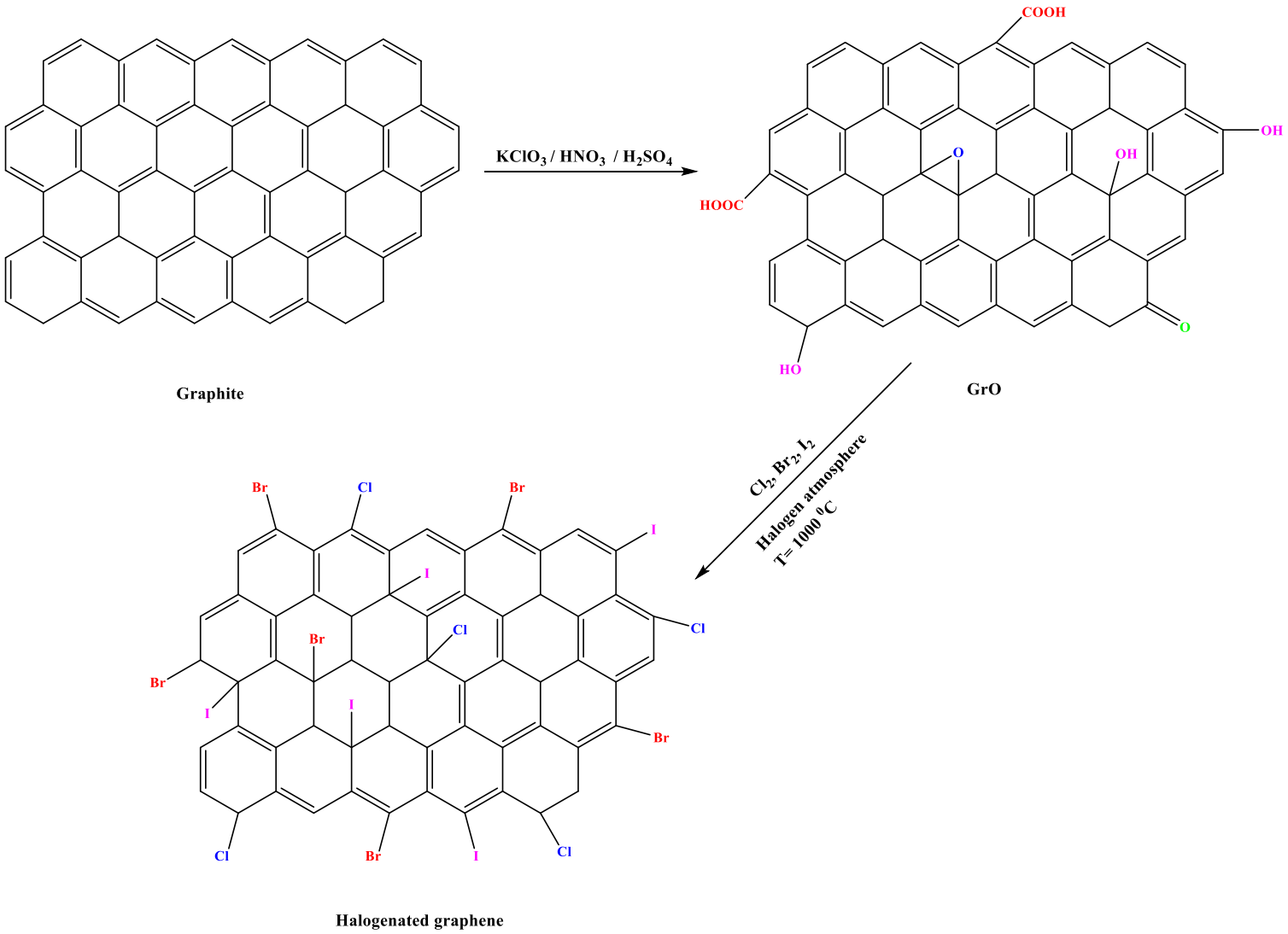

Fig. 7. Synthesis of halogenated graphene by thermal exfoliation of graphite oxide in a halogen atmosphere [117].

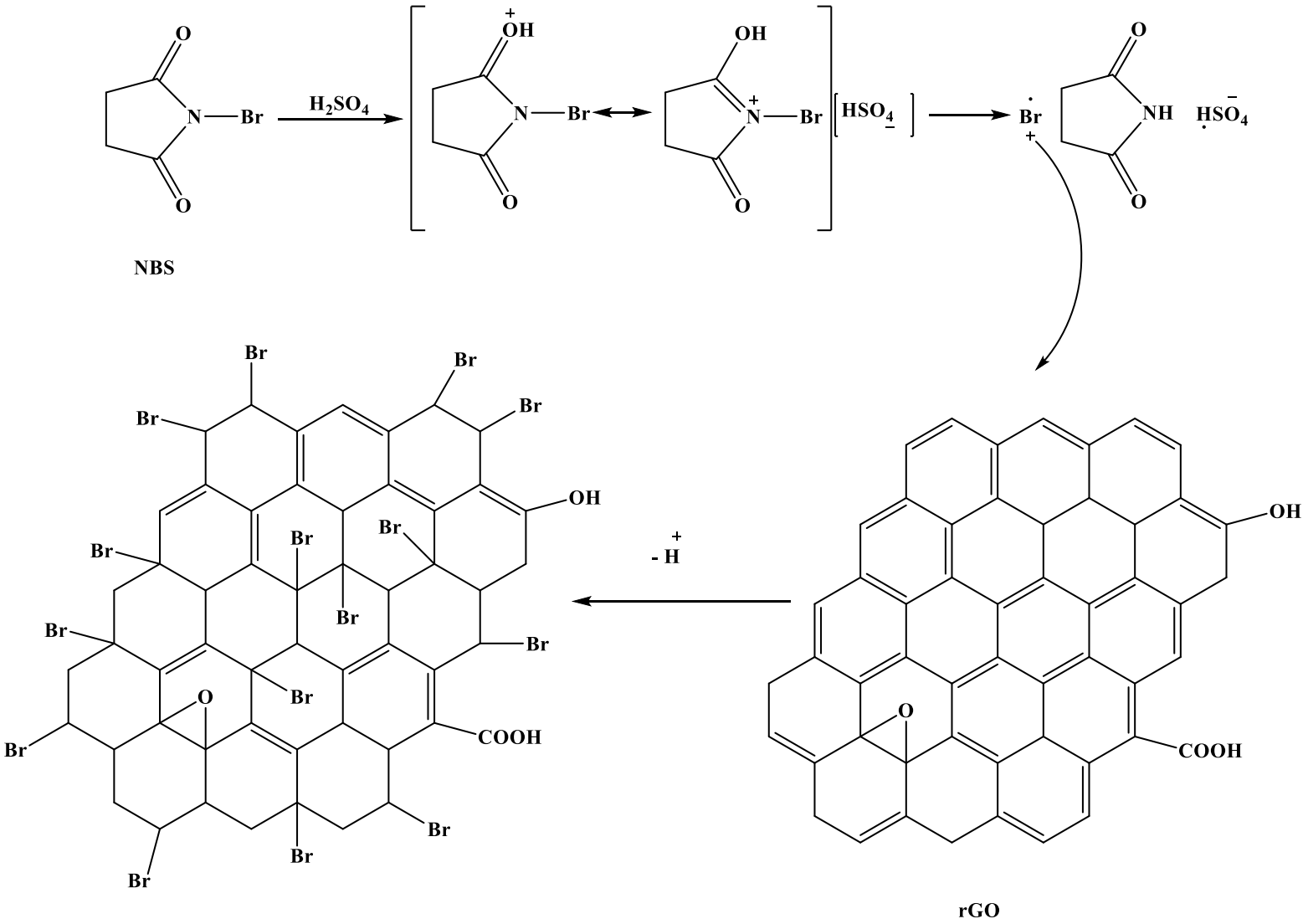

Fig. 8. Proposed mechanism of the bromination of RGO using NBS through electrophilic substitution reaction [118]

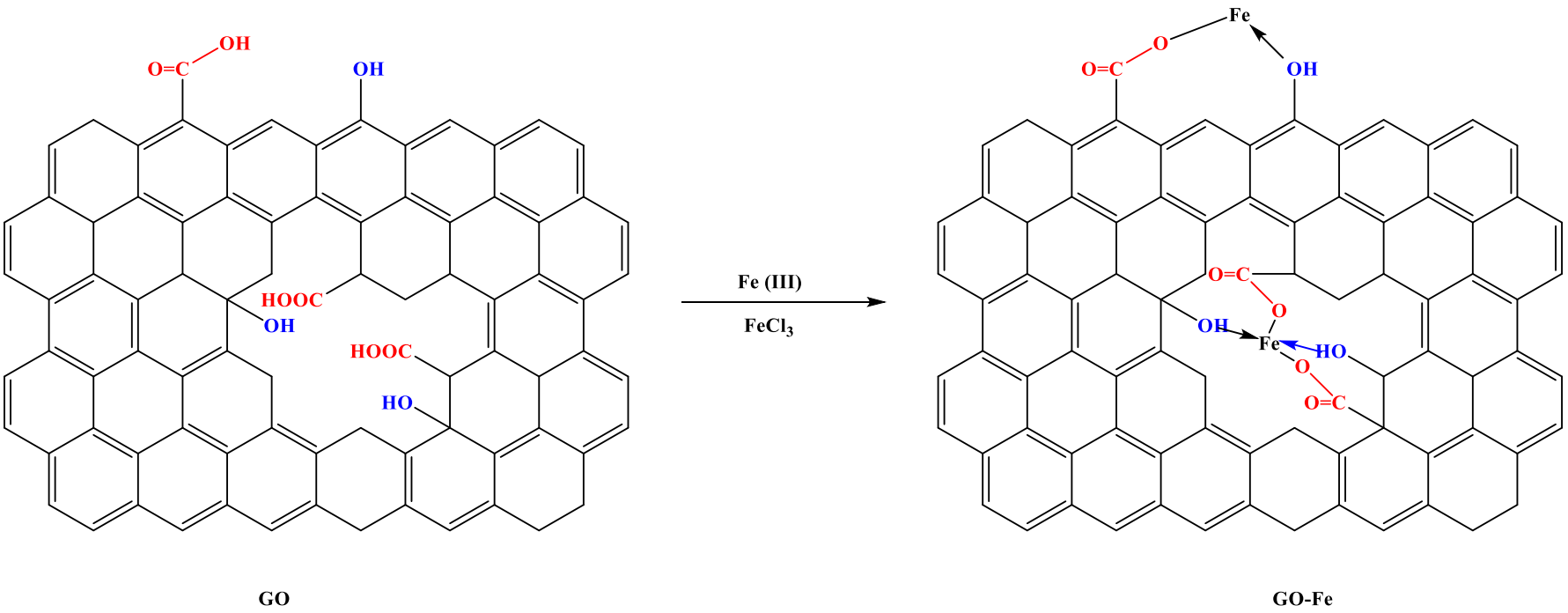

Fig. 9. Schematic illustration of the formation of GO–Fe complexes through oxygen-donor coordination of GO to ferric ions [119].

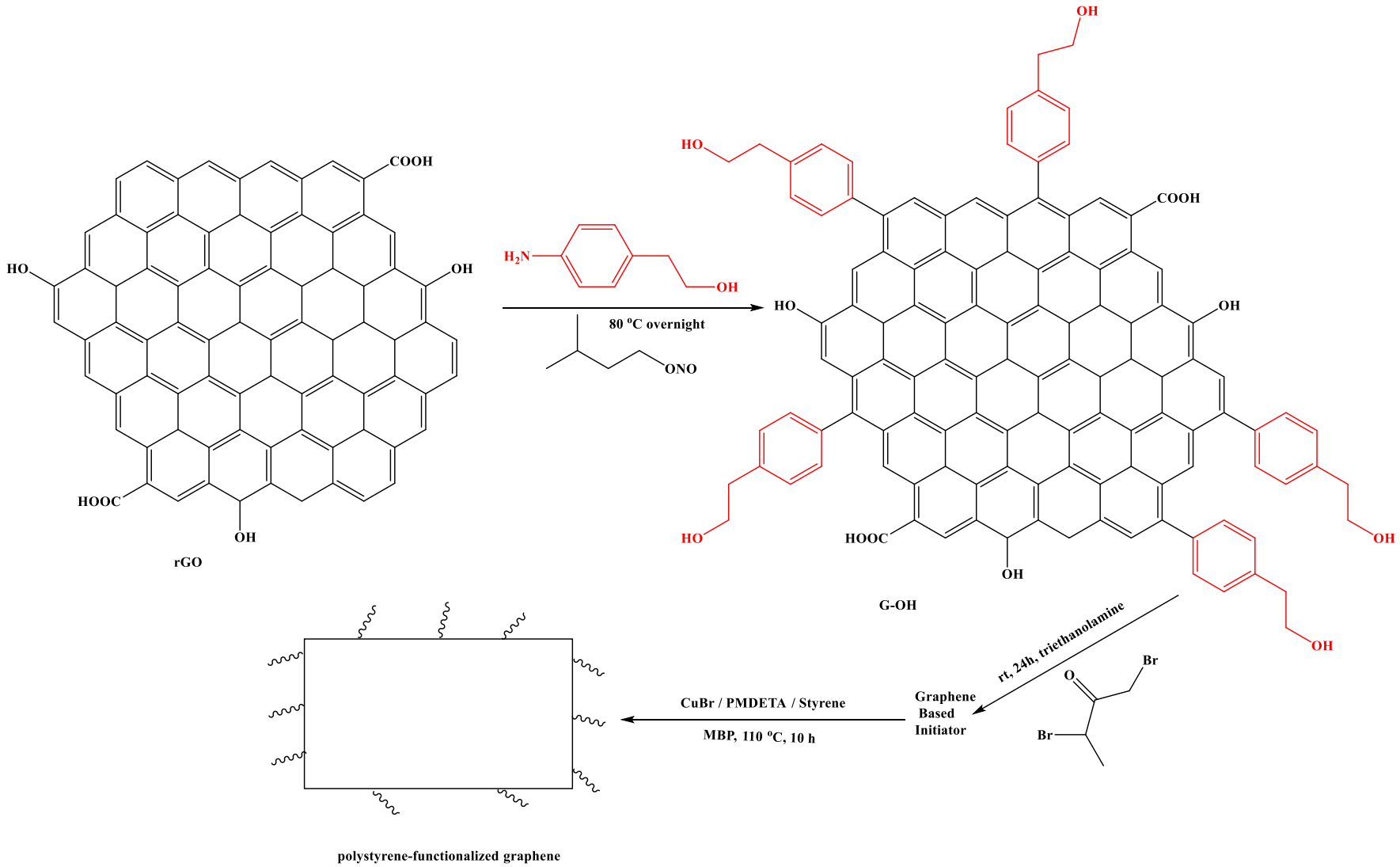

Fig. 10. Synthesis route of polystyrene-functionalised graphene nanosheets [159].

.

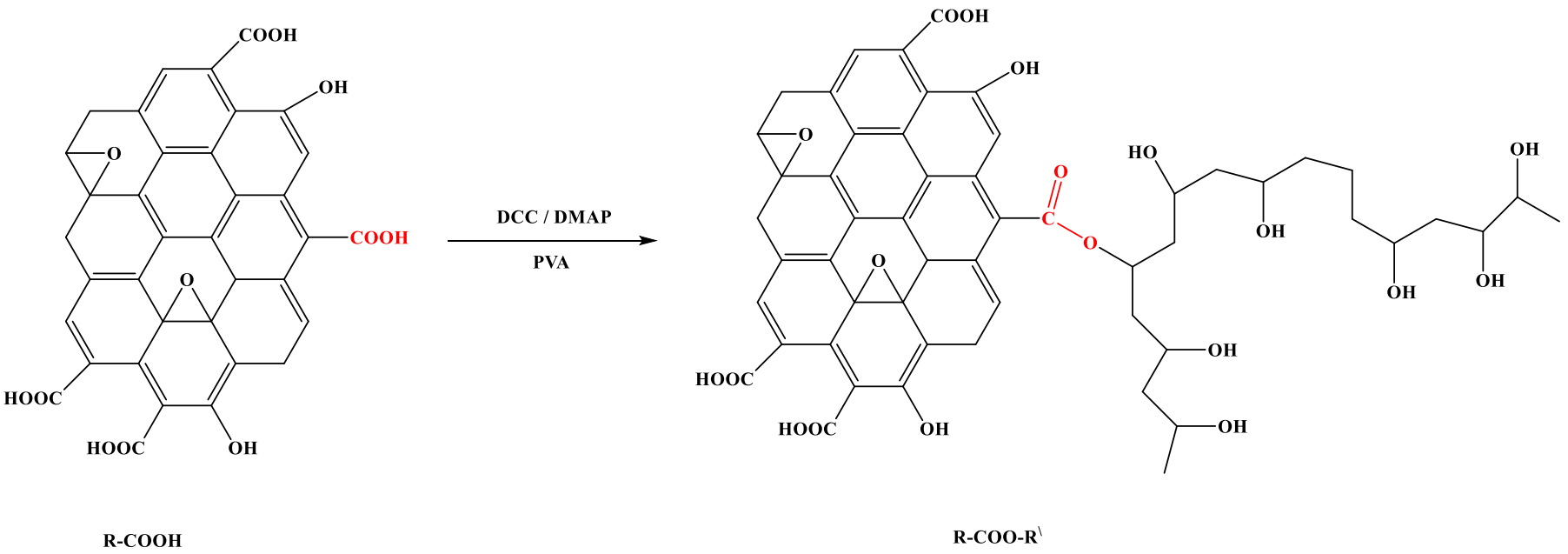

Fig. 11. Functionalisation of GO with poly(vinyl alcohol) by a carbodiimide esterification reaction [160].

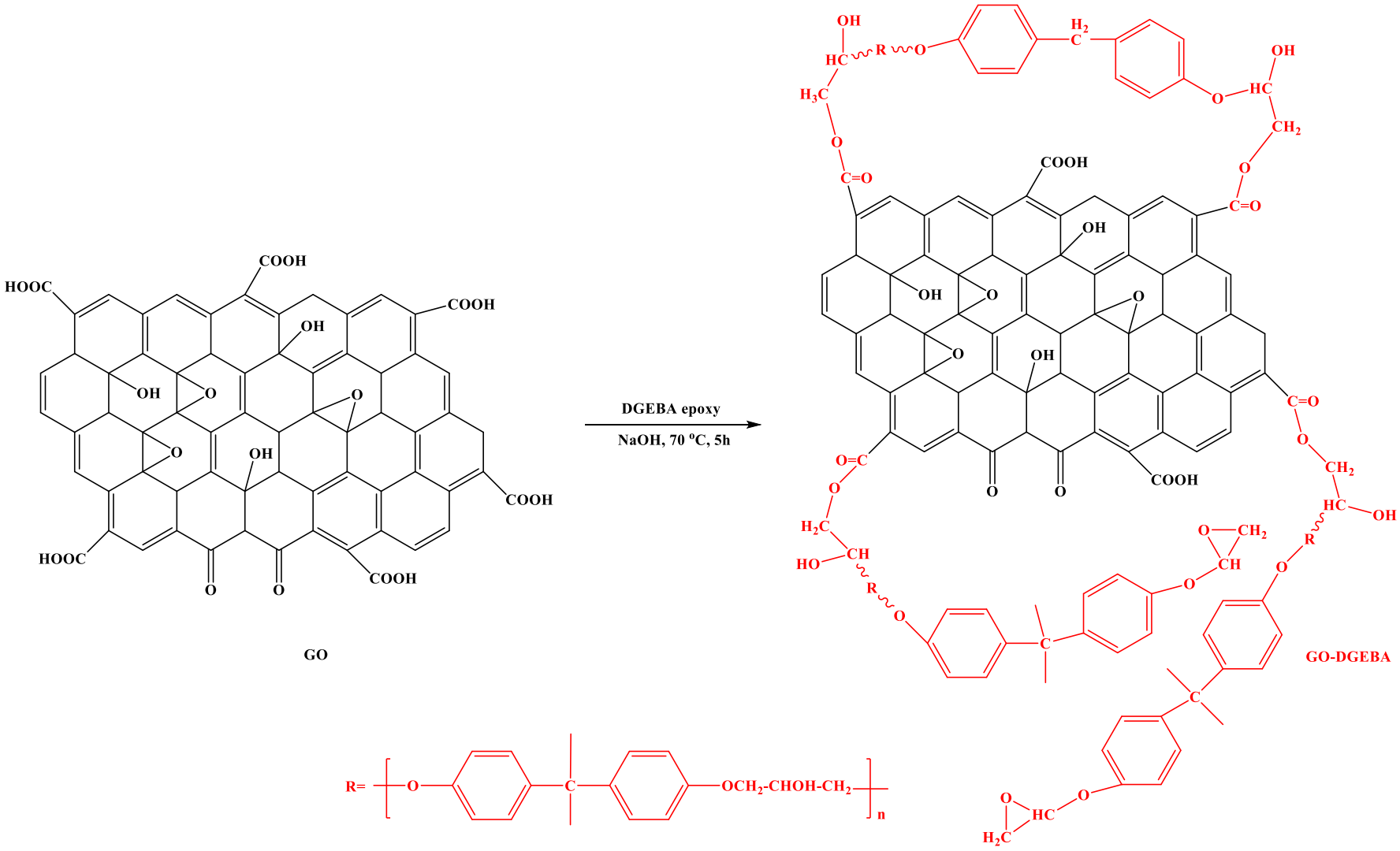

Fig. 12. Covalent functionalisation of GO with DGEBA [161].

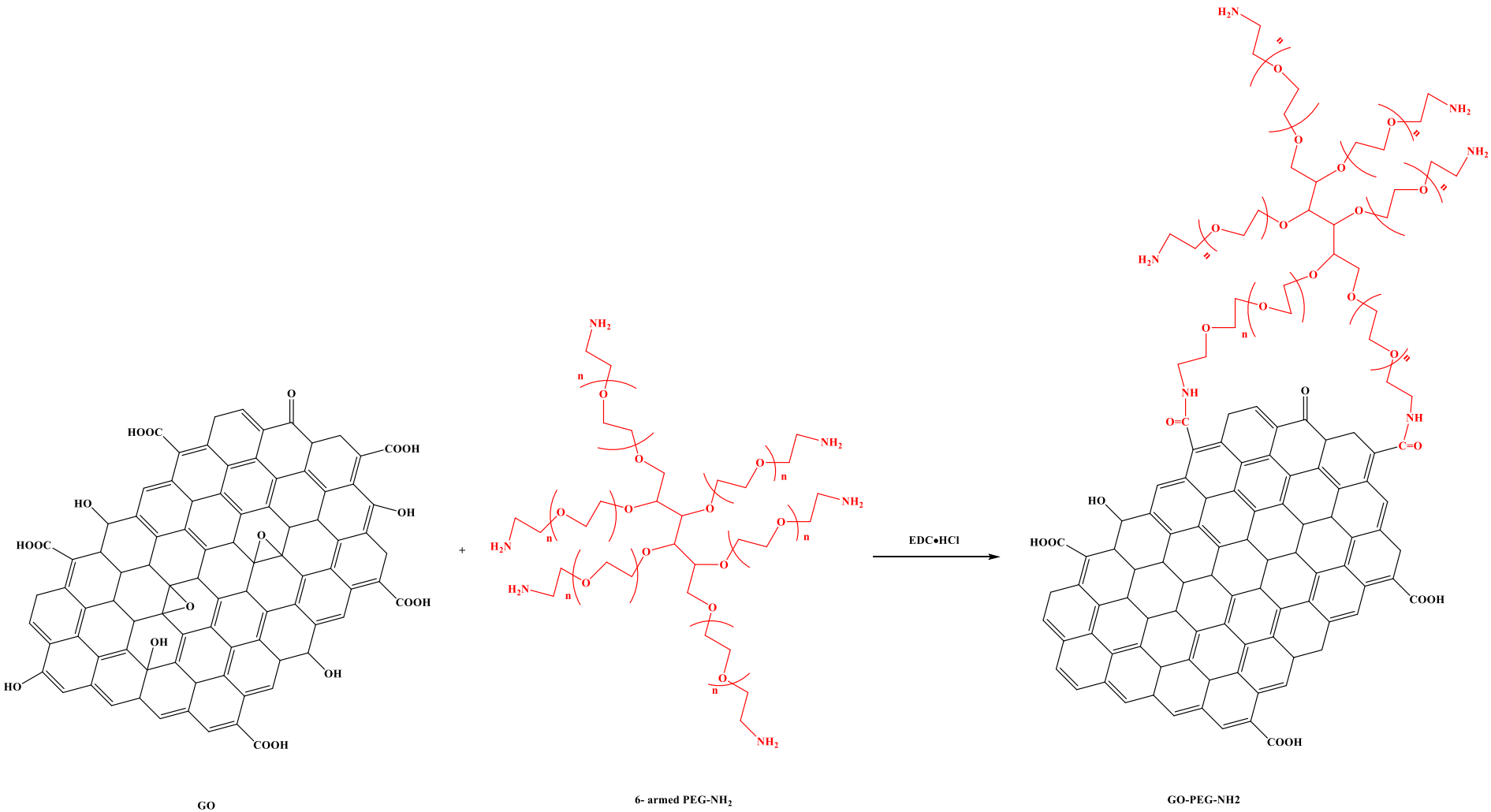

Fig. 13. Covalent functionalisation of GO with 6-armed PEG-NH_2 through amidation reaction [162]

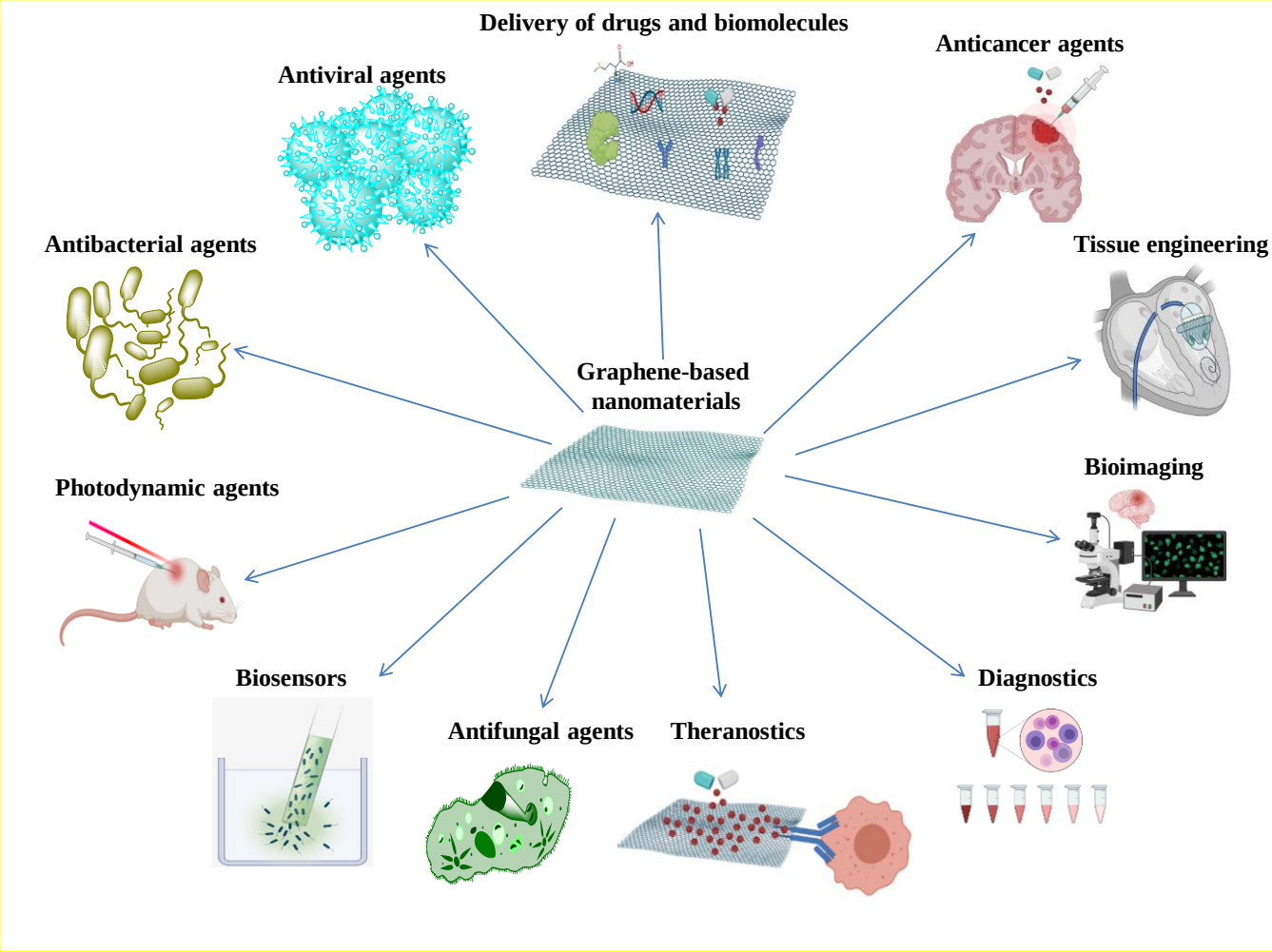

Fig. 14. The application of GBN in nanobiomedicine.